Food and Bioprocess Technology (2021) 14:831–853
https://doi.org/10.1007/s11947-021-02589-z

ORIGINAL RESEARCH

Anethum graveolens Essential Oil Encapsulation in Chitosan Nanomatrix: Investigations on In Vitro Release Behavior, Organoleptic Attributes, and Efficacy as Potential Delivery Vehicles Against Biodeterioration of Rice (*Oryza sativa* L.)

Somenath Das[1] · Vipin Kumar Singh[1] · Abhishek Kumar Dwivedy[1] · Anand Kumar Chaudhari[1] · Nawal Kishore Dubey[1]

Received: 14 July 2020 / Accepted: 19 January 2021 / Published online: 16 February 2021

Abstract

The study deals with first time report on encapsulation of chemically characterized *Anethum graveolens* essential oil within chitosan nanomatrix (Nm-AGEO) using ionic gelation technique to enhance the antimicrobial, antiaflatoxigenic, antioxidant, and in situ efficacy against stored rice biodeterioration. GC-MS analysis of AGEO revealed dill apiol (33.79%), carvone (27.19%), and limonene (13.76%) as major components. Nm-AGEO characterization through scanning electron microscopy (SEM), X-ray diffractometry (XRD), and Fourier transform infrared spectroscopy (FT-IR) confirmed successful encapsulation of AGEO within chitosan as an encapsulant. Biphasic and sustained release pattern reflected controlled volatilization of bioactives, helpful in shelf-life extension of stored food commodities. Nm-AGEO caused significant impairment in fungal ergosterol biosynthesis and enhanced leakage of vital ions indicating destabilization in plasma membrane integrity. Inhibition of methylglyoxal (aflatoxin inducer) biosynthesis by Nm-AGEO confirmed novel antiaflatoxigenic mechanism of action, suggesting its future exploitation for development of aflatoxin-resistant rice varieties through green transgenics. Nm-AGEO induced impairment in antioxidant defense enzymes (SOD, CAT) and non-enzymatic defense biomolecules GSH and GSSG revealing biochemical mechanism of action. In silico modeling of carvone and limonene with *Omt-A* and *Ver-1* genes suggested molecular mechanism of aflatoxin inhibition. Treatment of rice samples with Nm-AGEO caused significant protection from aflatoxin B_1 contamination and lipid peroxidation without altering organoleptic properties. Moreover, favorable safety profile for mammalian system and non-phytotoxic nature of chitosan-fabricated AGEO nanoemulsion-based delivery system recommend attention of food industries for its formulation as potential green preservative.

Keywords *Anethum graveolens* essential oil · Nanoemulsion · Antimicrobial · Aflatoxin B_1 · Molecular docking

Introduction

Currently, increasing contamination of stored foods by fungi and their associated mycotoxin is a major challenge for food safety. Rice (*Oryza sativa* L.), by virtue of its sovereign nutritional properties (proteins, fats, carbohydrates, minerals, and vitamins) and antioxidant activities, has been recognized as staple food as well as pharmaceutical adjuvant throughout the world (Liu et al. 2020). However, unlike other agricultural commodities, rice seeds are biodeteriorated by infestation of toxigenic species of *Aspergillus*, *Penicillium*, and *Fusarium* producing several toxic metabolites (mycotoxins), especially in the tropical and subtropical zones across the globe (Ali 2019). Among different food contaminating mycotoxins, aflatoxin B_1 (AFB_1) secreted by *A. flavus*, *A. parasiticus*, and *A. nomius* has been considered as potent carcinogen and mutagen. Methylglyoxal, a respiratory byproduct produced during metabolic processes has been reported to induce aflatoxin biosynthesis and reduce the shelf-life of stored food commodities (Das et al. 2021a). In addition to fungal and aflatoxin contamination, lipid peroxidation in stored food commodities

Somenath Das and Vipin Kumar Singh contributed equally to this work.

✉ Nawal Kishore Dubey
nkdubeybhu@gmail.com

[1] Centre of Advanced Studies in Botany, Institute of Science, Banaras Hindu University, Varanasi 221005, India

deteriorates the food quality leading to unpleasant odor, formation of toxic hydro-peroxides, rancidity, off-flavor, and reduction in vital nutritional constituents (Liu et al. 2017). Currently, the inhibition of fungal growth and subsequent mycotoxin contamination through indiscriminate application of synthetic preservatives has emerged as a matter of increased concern. In addition, commonly used synthetic preservatives viz phosphine, organophosphates, methylbromide, BHT, and BHA have shown ill effect on human health and environmental integrity and most importantly the development of resistant fungal races (Cao et al. 2019).

Utilization of plant essential oils for stored food preservation as an efficient alternative of synthetic preservatives is currently gaining noticeable momentum and a number of essential oil-based formulations such as Ecotrol, DMC base natural, and TALENT are being used as green preservatives. Essential oils possess diverse bioactive components with remarkable antifungal, antimycotoxigenic, antibacterial, and antiviral activities representing multi-target mechanism of action and considered under generally recognized as safe (GRAS) category, thereby with negligible chance of resistance development in target pests (Hemmatkhah et al. 2020). Moreover, molecular interaction of different bioactive components of essential oils with a variety of regulatory genes leading to inhibition of AFB_1 biosynthesis through conformational changes has been recently reported (Murugan et al. 2013). However, under natural condition, the antimicrobial property of essential oil is significantly affected by different environmental factors such as temperature, light, moisture, pH, and oxygen facilitating cyclization, isomerization, oxidation, and dehydration reactions which ultimately lead to limited solubility and dispersion as well as uncontrolled and rapid release of essential oils in food system. Also, the direct application of essential oils in food system may cause unacceptable changes in organoleptic attributes of food materials limiting their large-scale application in food and agricultural industries (Ezhilarasi et al. 2013).

To overcome such drawbacks, nanoencapsulation of essential oil into any metastable polymeric nanomatrix has emerged as a suitable alternative resulting into enhanced biological efficacy, physical stability, and protection from humidity, oxygen, light, and mobility of the components inhibiting lipid peroxidation with undesirable effects in food system (Ghaderi-Ghahfarokhi et al. 2016). Moreover, encapsulation facilitates the controlled release of bioactive components ensuring maintenance of nutritional, organoleptic properties, and possible enhancement in food shelf-life (Oliveira et al. 2018). In comparison to other encapsulation strategies, nanoemulsion produced by ionic gelation is a valid and feasible approach in terms of nanorange particles with greater surface to volume ratio, increased solubility, decreased volatility, and controlled release properties (Chaudhari et al. 2020). To date, large numbers of natural biopolymers viz whey protein, gelatin, soy protein, sodium caseinate, gum arabic, starch, maltodextrin, inulin, fructan, and chitosan have been used (Oliveira et al. 2018); among them, chitosan (1,4-2-amino-2-deoxy-glucopyranose) with functional groups like hydroxyl and amine facilitate intermolecular interaction with negatively charged polyphosphate groups of sodium tripolyphosphate (S-TPP) during ionic gelation resulting from polar nature with excellent biocompatibility, biodegradability, and environmental acceptance has attracted wide attention for encapsulation of essential oils (Gómez-Pastora et al. 2014; Hasheminejad et al. 2019). Different methods have been used for encapsulation of essential oils and bioactive components; however, ionic gelation is much commonly preferred technique for encapsulation of essential oil because the process is free of excessive organic solvent, appropriate, controllable, non-toxic and is largely based on the electrostatic interaction between free amine groups of chitosan with polyanions of S-TPP (Esmaeili and Asgari 2015).

Anethum graveolens L., commonly known as "dill plant," grows abundantly in Mediterranean regions of Asia and southeastern zones of Europe and is commonly used as flavoring agent for foods, and beverages. *Anethum graveolens* seed essential oil (AGEO) possesses different pharmacological properties like antidiabetic, anticancer, antisecretory, antihyperlipidemic, antifungal, and significant ability to relieve gastrointestinal disorders, mental complaints, and menstrual imbalance and promote milk secretion in lactating mother (Kaur et al. 2019). To date, various literature on AGEO indicating its antifungal efficacy have been published; however, the literature is completely lacking on underlying biochemical and in silico mechanisms of action for inhibition of fungal infestation, AFB_1 secretion, lipid peroxidation, and enhancement in bioefficacy through nanoencapsulation technology for protection of stored rice as an efficient safe and green preservative in food and agriculture industries.

Hence, the major objective of this investigation was to study the fungitoxicity, AFB_1 inhibitory action, antioxidant potency, and enhancement in overall bioefficacy of AGEO through nanoencapsulation within chitosan biopolymer. Physico-chemical characterization of nanoencapsulated AGEO was done through scanning electron microscopy (SEM), X-ray diffraction (XRD) and Fourier transform infrared spectroscopic (FT-IR) analysis. In vitro release behavior has been investigated to determine the controlled release of AGEO having advantageous efficacy in improving the shelf-life of stored food products. Further, the speculated biochemical mode of action in terms of membrane stability, methylglyoxal biosynthesis and effect on different enzymatic as well as non-enzymatic antioxidant defense molecules has also been investigated. In silico modeling of carvone and limonene with AFB_1 regulatory genes *Omt-A* and *Ver-1* were performed to determine the molecular mechanism of antiaflatoxigenic activity. In addition, practical application in

terms of in situ efficacy on rice (the model food system), lipid peroxidation, antioxidant activity, phytotoxicity assay, and sensorial evaluation (effect on organoleptic property of the model food) has been investigated to explore the prospects of nanoencapsulated AGEO in food and allied industries as eco-friendly preservative.

Materials and Methods

Chemicals, Solvents, and Microbial Media

Chemicals viz methanol, isoamyl alcohol, anhydrous sodium sulfate (Na_2SO_4), Folin–Ciocalteu reagent, SMKY (sucrose, 200 g; $MgSO_4$ $7H_2O$, 0.5 g; KNO_3, 0.3 g; yeast extract, 7 g), potato dextrose agar (PDA), chitosan, thiobarbituric acid (TBA), tricholoroacetic acid (TCA), phosphate buffer, HCl, acetonitrile, acetone, dichloromethane, KOH, *n*-heptane, NaCl, S-TPP, phosphoric acid, perchloric acid ($HClO_4$), propidium iodide (PI), ethanol, $K_2S_2O_8$, K_2CO_3, Tween 80, Tween 20, DMSO, NaOCl, Na_2CO_3, methylglyoxal, 1,2 diaminobenzene (DAB), quercetin, dichloro-dihydro-fluorescein diacetate (DCFH-DA), acetic acid, gallic acid, DPPH, and ABTS were procured from Hi-media laboratories, Mumbai, India.

Isolation and GC-MS Analysis of Essential Oil

Dried seeds of *Anethum graveolens* were collected from botanical garden of Banaras Hindu University, India. One thousand grams of dried seeds were placed in Clevenger's hydro-distillation apparatus having a heating mantle and a cooling system for 4 h. Extracted AGEO was passed over Na_2SO_4 to remove water traces.

AGEO was characterized through Thermo Scientific-1300 TSQ Duo triple quadruple fitted gas chromatography–mass spectrometry (Perkin Elmer Turbomass Gold MA, USA). Briefly, 1 μL of AGEO was injected into TG-5 MS capillary column (30 m × 0.25 mm ID × 0.25 μm thickness) having the injector temperature at 280 °C and splitting ratio of 1:50. Helium was utilized as carrier gas. Oven and transfer line temperature was set according to the standard protocol of Adams (2017). Major components of AGEO were identified based on the similarity of spectral fragmentation, retention time, and peak alignment of different libraries such as Wiley (WILEY7.LIB), NIST (NIST-17), NBS, FFNSC-2, and other published literature data.

Test Fungal Strain

Aflatoxigenic strain of *Aspergillus flavus* (AF LHP R14) and different food contaminating molds viz *A. niger*, *A. candidus*, *A. sydowii*, *A. fumigatus*, *A. repens*, *A. luchuensis*, *F. poae*, *F. oxysporum*, *Cladosporium herbarum*, *Curvularia lunata*, *Alternaria alternata*, *A. humicola*, and Mycelia sterilia isolated during mycoflora analysis of rice samples were used for the study (Das et al. 2020a). Spore suspension of AF LHP R14 strain was prepared in 0.1% aqueous Tween 80 solution (spore density = 10^6 spores/mL) and kept at 4 °C in refrigerator.

Chitosan-Fabricated AGEO Nanoemulsion (Nm-AGEO) Preparation

Nm-AGEO was prepared according to the protocol used by Hosseini et al. (2013) with some modifications. 1.5 g chitosan was dissolved in 100 mL acetic acid (1%) followed by addition of Tween 80 as surfactant and stirred for 2 h at 45 °C. Different proportion of AGEO mixed with dichloromethane (4 mL) was added into chitosan solution at the time of homogenization (12,000×*g* for 12 min) using IKA, T18ED, homogenizer, Germany. S-TPP solution (0.4%) was dropped into homogenized chitosan solution, and after proper mixing, the emulsion was centrifuged at 12,000×*g* for 12 min followed by repeated washing with deionized water for 2–3 times. The collected pellet was again dissolved in deionized water followed by ultra-sonication (Sonics, Vibra Cell) for 4 min (1 min pulse on; 1 min pulse off). Different ratio of chitosan to AGEO (w/v) (1:0, 1:0.2, 1:0.4, 1:0.6, 1:0.8, 1:1) was prepared to analyze the maximum loading of AGEO within chitosan matrix. Similar procedure without addition of AGEO was done for preparation of chitosan nanoemulsion. Emulsion was lyophilized using freeze dryer (Alpha 1–2LD, plus model, Sydney, Australia) for physico-chemical characterizations.

Physico-chemical Characterization

Scanning Electron Microscopic Observation

External morphology of chitosan nanoparticle and Nm-AGEO nanoparticle was observed in SEM (EVO 18 Research, Zeiss, Germany) after gold coating under vacuum. One drop of water suspended nanoparticles was spread over cover slip and dried in sterile air followed by observation under SEM with detector at 15 kV acceleration voltage and 50,000 to 70,000× magnification.

Fourier Transformed Infrared Spectroscopic Investigation

FT-IR investigation of chitosan, AGEO, chitosan nanoparticle, and Nm-AGEO nanoparticle was performed in Perkin Elmer Fourier transform infrared spectrometer (IR Affinity-1, Shimadzu, Japan) in between 400 and 4000 cm^{-1} having 64 scans with resolution at 4 cm^{-1}.

X-ray Diffraction Investigation

XRD investigation of chitosan, chitosan nanoparticle, and Nm-AGEO nanoparticle was performed in X-ray diffractometer (Bruker Advance, Germany) employing Cu-Kα as X-ray source and scanned over 5–50° of 2θ ranges having the scanning rate of 5° min^{-1}.

Encapsulation Efficiency (EE), Loading Capacity (LC), and Nanoparticle Yield (NY) of Nm-AGEO

Amount of AGEO in chitosan nanoemulsion was measured spectrophotometrically at λ_{max} 285 nm prepared in ethyl acetate. Briefly, 300 μL of Nm-AGEO of different chitosan to AGEO ratio (w/v) was mixed properly in 3 mL of ethyl acetate followed by centrifugation at 12,000×g for 15 min. Blank sample for chitosan nanoemulsion did not possess AGEO. Optical density was recorded at 285 nm according to the standard calibration curve of AGEO. Percent LC and EE were determined from the following equations.

$$\%\mathrm{LC} = \frac{\text{Total amount of AGEO}}{\text{Initial amount of AGEO}} \times 100 \quad (1)$$

$$\%\mathrm{EE} = \frac{\text{Total amount of loaded AGEO}}{\text{Weight of nanoemulsion}} \times 100 \quad (2)$$

Percent NY was determined for only at maximum loading of chitosan to AGEO (1:0.8 w/v ratio) by the following formula:

$$\%\mathrm{NY} = \frac{\text{Amount of freeze dried nanoparticle}}{\text{Sum total of all the individual components}} \times 100 \quad (3)$$

Release Tests of Nm-AGEO

Release tests were studied by dissolving 300 μL of Nm-AGEO (1:0.8 ratio) into 5 mL of phosphate-buffered saline (PBS) and ethanol (100%) mixture followed by incubation for 7 days. After proper shaking and centrifugation, 300 μL of upper layer was extracted and absorbance was measured at 285 nm under ambient temperature (25 °C) condition at specific time intervals. Each and every time after collection of the upper layer, total volume was kept constant by adding PBS. Cumulative release of AGEO was calculated by the following formula:

$$\text{Cumulative release of AGEO}\,(\%) = \frac{\text{Cumulative amount of AGEO released at each time}}{\text{Initial amount of AGEO loaded in sample}} \times 100 \quad (4)$$

Fungitoxicity and AFB_1 Inhibitory Activity of AGEO and Nm-AGEO: In Vitro Investigation

In vitro antifungal efficacy of AGEO and Nm-AGEO against toxigenic AF LHP R14 strain was tested in liquid SMKY medium. Required volumes of AGEO (0.2–1.2 μL/mL) and Nm-AGEO (0.1–0.6 μL/mL) were added into 25 mL SMKY followed by inoculation of 25 μL AF LHP R14 spore suspension and incubation up to 10 days at 25 ± 2 °C. Two different control sets viz chitosan nanoemulsion (chitosan content equivalent to highest effective AGEO concentration) and Tween 20 solution (5%) mixed with SMKY were prepared. After completion of incubation periods, the concentrations showing complete inhibition of the visible growth of fungal strain were selected as minimum inhibitory concentrations (MICs). Fungitoxic spectrum of AGEO and Nm-AGEO was also tested against 14 food biodeteriorating molds viz. *A. niger*, *A. candidus*, *A. sydowii*, *A. fumigatus*, *A. repens*, *A. luchuensis*, *F. poae*, *F. oxysporum*, *Cladosporium herbarum*, *Curvularia lunata*, *Alternaria alternata*, *A. humicola*, and Mycelia sterilia at the MIC dose (1.2 and 0.6 μL/mL) by inoculation of 5 mm disc of each mold in PDA medium. Percent inhibition of mold growth was calculated based on the suppressing potentiality of colony diameter using the following formula

$$\%\text{inhibition} = \frac{\text{Diameter of mold colony in control} - \text{Diameter of mold colony in treatment}}{\text{Diameter of mold colony in control}} \times 100 \quad (5)$$

Quantification of AFB_1 was done by separating the culture media through sterilized muslin cloth followed by extraction in $CHCl_3$, evaporation, and the residue dissolution in methanol. Dissolved residue (25 μL) was loaded on the thin-layer chromatographic (TLC) plate and run using the solvent system of methanol, toluene, and isoamylalcohol (2:90:32 v/v/v). Blue spots (as observed in UV transilluminator) were scrapped, added into methanol and centrifuged at 3000×g for 5 min. The supernatant was used for analysis of AFB_1 content at 365 nm by using the following formula:

$$\mathrm{AFB_1\ content}(\mu g/\mathrm{mL}) = \frac{\text{Absorbance} \times \text{Molecular weight of AFB}_1}{\text{Molar extinction coefficient of AFB}_1 \times \text{Path length}} \times 1000 \quad (6)$$

Concentration of AGEO and Nm-AGEO causing total inhibition of AFB_1 was recorded as minimum aflatoxin B_1 inhibitory concentration (MAIC).

Effect of AGEO and Nm-AGEO on Spore Germination of AF LHP R14 Strain

MIC concentrations of AGEO and Nm-AGEO were added into 10 mL of SMKY medium followed by addition of 10 μL of AF LHP R14 spore suspension. Controls were devoid of AGEO and Nm-AGEO. All the sets were incubated at 25 ± 2 °C for 24 h. Spore germination was seen under compound microscope at 400× magnification. Effective inhibition of germ tube formation was expressed with respect to control according to the following formula

$$\%\text{Inhibition of spore germination} = \frac{\text{Average number of spore germinated in control} - \text{average number of spore germinated in treatment}}{\text{Average number of spore germinated in control}} \times 100 \quad (7)$$

Biochemical and Molecular Mechanism of Action of AGEO and Nm-AGEO

Effect of AGEO and Nm-AGEO on Membrane Stability and Integrity of AF LHP R14 Cells

Effect of AGEO and Nm-AGEO on plasma membrane stability of AF LHP R14 strain was determined by ergosterol quantification assay. Desired amount of AGEO (0.2–1.2 μL/mL) and Nm-AGEO (0.1–0.6 μL/mL) was dissolved separately in 25 mL SMKY medium and inoculated with 10 μL AF LHP R14 spores. Control did not possess AGEO and Nm-AGEO. After 4 days of incubation, wet weight of mycelia was determined and suspended into KOH solution. The mixture was heated at 85 °C for 2 h. Subsequently, distilled water and *n*-heptane mixture (2:5 v/v) was added to each mycelial biomass and vortex mixed for 3 min for separating two distinct layers. Upper clear layer was decanted and scanned between 230 and 300 nm by UV-visible spectrophotometry. Presence of ergosterol and late sterol intermediate 24 (28) dehydroergosterol indicated the four-peaked curve, while the flat line demonstrated the absence of detectable ergosterol. Ergosterol content was determined by the formula of Tian et al. (2012).

$$\%\text{Ergosterol} + \%24\ (28)\ \text{dehydroergosterol} = \left(\frac{\text{Absorbance at 281.5 nm}}{290} \times F\right)/\text{Pellet weight} \quad (8)$$

$$\%24\ (28)\ \text{dehydroergosterol} = \left(\frac{\text{Absorbance at 230 nm}}{518} \times F\right)/\text{Pellet weight} \quad (9)$$

$$\%\text{Ergosterol} = (\%\text{Ergosterol} + \%24\ (28)\ \text{dehydroergosterol}) - (\%24\ (28)\ \text{dehydroergosterol}) \quad (10)$$

where F = factor for dilution in *n*-heptane, and 290 and 518 are E values (percentage/cm) for ergosterol and 24 (28) dehydroergosterol.

Propidium iodide (PI) is a standard chemical reagent which helps in assessing the viable cells and excludes the non-viable ones. Propidium iodide specifically binds with double-stranded DNA of viable cells upon the disintegration of plasma membrane; thus, intensity of fluorescence directly represents the level of membrane damage. Hence, the determination of membrane integrity after AGEO and Nm-AGEO fumigation by using the propidium iodide is an important parameter of our study. Membrane integrity was determined at ½ MIC, MIC and 2 MIC doses of AGEO and Nm-AGEO in PBS solution. Three hundred milligrams of mycelial biomass (harvested from 7 days old AF LHP R14 biomass) was subjected for fumigation at ½ MIC, MIC and 2 MIC doses of AGEO and Nm-AGEO followed by incubation at 25 ± 2 °C for 24 h. After proper washing, the obtained biomass was washed by PBS, followed by staining with propidium iodide for 15 min at ambient temperature. Subsequently, the biomass was collected, washed, crushed in 2 mL of PBS, and centrifuged at 12,500×*g* for 15 min. Fluorescent intensity of collected supernatant was recorded at excitation and emission wavelength of 546 and 590 nm, respectively. Effect of AGEO and Nm-AGEO on efflux of cellular cations (Mg^{2+}, Ca^{2+}, K^{+}) and 260 and 280 nm absorbing materials was determined in 0.85% NaCl solution by using atomic absorption spectroscopy (Aanalyst 800, Perkin Elmer, USA) and UV-visible spectrophotometer (Shimadju 2900), respectively (Das et al. 2019).

Effect of AGEO and Nm-AGEO Against Cellular Methylglyoxal (MG) Biosynthesis

Three hundred milligrams biomass of AF LHP R14 cells (7 days grown) was suspended separately in 10 mL SMKY medium and fumigated with ½ MIC, MIC, and 2 MIC concentrations of AGEO and Nm-AGEO followed by incubation at 25 ± 2 °C for 16 h. Thereafter, biomass was crushed into 3 mL of chilled $HClO_4$ followed by centrifugation at 10,000×*g* for 12 min and collected supernatant was neutralized with saturated solution of K_2CO_3. Quantification of MG was done by subsequent mixing of DAB (0.072 M), $HClO_4$ (5 M), and

supernatant and absorbance of the reaction mixture was recorded at 336 nm (Yadav et al. 2005). Amount of cellular MG was calculated by comparing the absorbance value with standard calibration curve of MG (10–100 μM) prepared in double-distilled water.

In Silico Modeling of Carvone and Limonene with AFB_1 Biosynthetic Regulatory Genes *Ver-1* and *Omt-A*: Molecular Mechanism of Action

Peptide sequences of Ver-1 and Omt-A of *Aspergillus flavus* were retrieved in FASTA format from UNIPROT (https://www.uniprot.org/) protein database and 3D structures of carvone and limonene were downloaded in SDF format from PUBCHEM (https://pubchem.ncbi.nlm.nih.gov/) database. Phyre-2 online server was used to generate 3D model of the proteins. Molecular docking of limonene and carvone with Ver-1 and Omt-A proteins was done in PATHCHDOCK online tool. The best 20 models were further refined by using FIRE-DOCK. Selection of the best structures based on global energy, attractive van der Waals force (VdW), repulsive van der Waals force (VdW), and atomic contact energy (ACE) was done through PYMOL and CHIMERA 1.8.1 software (Das et al. 2021b).

Effect of AGEO and Nm-AGEO on Enzymatic and Non-enzymatic Antioxidative Defense in AF LHP R14 Cells

AGEO and Nm-AGEO-fumigated (½ MIC, MIC and 2 MIC) biomass of AF LHP R14 strain was crushed into 3 mL PBS followed by centrifugation at 8000×*g* for 20 min. Supernatant was used for analysis of different enzymatic and non-enzymatic antioxidative biomolecules. Cellular reactive oxygen species (ROS) was determined by DCFH-DA at 485 and 530 nm. Level of ROS was expressed in terms of μM/mg protein. Determination of Catalase (CAT) activity was measured at 240 nm and the amount was expressed as unit activity/mg protein. Superoxide dismutase (SOD) was measured through quercetin auto-oxidation methods at 406 nm at 0 and after 20 min and the amount was expressed in unit activity/mg protein. For estimation of glutathione (reduced and oxidized; GSH/GSSG), absorbance of the supernatant was measured at 420 and 350 nm (Das et al. 2021a). Amount of cellular reduced and oxidized glutathione was expressed in μM/mg protein. Protein content was determined through Lowry et al. (1951).

Total Phenolic Content and In Vitro Radical Scavenging Activity of AGEO and Nm-AGEO: $DPPH^{\cdot}$ and $ABTS^{\cdot+}$ Assay

Total phenolic content of AGEO and Nm-AGEO was determined through established protocol of Folin–Ciocalteu assay (Das et al. 2019). In case of $DPPH^{\cdot}$ free radical scavenging assay, different concentrations (2–20 μL/mL) of AGEO, chitosan nanoemulsion, and Nm-AGEO were mixed with 5 mL methanolic $DPPH^{\cdot}$ (0.004%) solution followed by incubation for 30 min (protected from light). Absorbance at 517 nm was noted for determination of radical scavenging activity (RSA). $ABTS^{\cdot+}$ reaction mixture was prepared by mixing ABTS (7 mM) and $K_2S_2O_8$ (2.54 mM) followed by incubation under dark for 16 h. Required volumes (1–10 μL/mL) of AGEO, chitosan nanoemulsion and Nm-AGEO were added into 3 mL $ABTS^{\cdot+}$ solution followed by incubation for 10 min in dark. Absorbance was measured at 734 nm. Percent radical scavenging activity (RSA) was determined according to the given formula.

$$\%\mathrm{RSA} = \frac{\text{Absorbance of blank} - \text{Absorbance of sample}}{\text{Absorbance of blank}} \times 100 \quad (11)$$

Antioxidant activity was expressed as IC_{50} (50% radical scavenging potentiality) and calculated from graph made for concentration of sample versus scavenging activity.

Preservative Efficacy of AGEO and Nm-AGEO Against Fungal Infestation, AFB_1 Secretion, and Lipid Peroxidation in Stored Rice (the Model Food System): In Situ Observation

In our study, rice (Kala Joha variety) was selected as model food system because of its utilization as staple food grain and important source of carbohydrate, minerals, lipids, and fibers which provide suitable platform for excessive fungal infestation and AFB_1 contamination in postharvest conditions. Stored rice contaminated with AFB_1 facilitates the development of aflatoxin M_1 (AFM_1) causing severe baby food spoilage with potent carcinogenicity (Das et al. 2020a). Moreover, the foodborne fungal species as described in "test fungal strain" section were isolated from the Kala Joha rice variety; therefore, to evaluate the preservative efficacy of AGEO and Nm-AGEO for controlling the fungal and aflatoxin contamination through in situ observation is an important parameter of our study. In situ fungitoxic and AFB_1 inhibitory efficacy of AGEO and Nm-AGEO on fumigated rice seeds was determined after 1 year of storage. Fumigation setup was prepared in four sets; uninoculated control (only rice seeds), inoculated control (rice seeds + AF LHP R14 spore suspension), uninoculated treatment (rice seeds + treatment with MIC and 2 MIC doses of AGEO and Nm-AGEO), and inoculated treatments (rice seeds + AF LHP R14 spore suspension + treatment with MIC and 2 MIC doses of AGEO and Nm-AGEO). Antifungal efficacy against *A. flavus* was analyzed through serial dilution. One gram of grinded rice samples was mixed with 10 mL of

deionized water and 1 mL of 10^{-4} dilution was inoculated in PDA medium. Determination of percent protection was calculated on the basis of following equation.

$$\%\text{Protection} = \frac{\text{Fungal colony in control set} - \text{Fungal colony in treated set}}{\text{Fungal colony in control set}} \times 100 \quad (12)$$

For determination of AFB_1 level in stored rice seeds, 5 g of finely grinded rice seeds was added into aqueous methanol followed by centrifugation at 9000×*g* for 5 min. Upper layer was diluted in chloroform and KBr-mixed distilled water and again centrifuged. Finally, the supernatant was dried over water bath (70 °C for 2 h), mixed with 50 μL methanol and analyzed through high-performance liquid chromatography (HPLC) (Waters, India). AFB_1 content was analyzed by using the solvent system consisting of water/methanol/acetonitrile (64:17:19 v/v/v) with 1 mL/min flow rate in C-18 reverse phase column and detected through photodiode array (PDA) detector at 365 nm followed by comparison with AFB_1 calibration curve (25–1000 ng/100 μL). The value of AFB_1 was expressed as μg/kg of rice sample.

Evaluation of lipid peroxidation in stored rice was done by determining the level of malondialdehyde (MDA) following the TBARS method of Das et al. (2019). One gram of well-grinded rice samples was mixed with 0.25% TBA and 10% TCA solution followed by addition of 0.25 N HCl. The obtained mixture was kept in water bath at 85–95 °C to develop red pink chromogen. Subsequently, the mixtures were cooled followed by centrifugation at 9500×*g* for 10 min. Optical density of extracted supernatant was measured at 532 nm and subtracted for the non-specific turbidity value at 600 nm to determine actual MDA level. The MDA content was determined on the basis of extinction coefficient of 155 mM^{-1} cm^{-1} and expressed as μM/gFW.

Sensory Attribute of AGEO and Nm-AGEO on Rice Seeds: Evaluation of Organoleptic Property

Sensory attribute/organoleptic property (visible appearance of color, texture, flavor, and odor) of rice seeds fumigated with AGEO and Nm-AGEO was measured by testing through 10 different unskilled consumers (5 men and 5 women) aged 25–40 years, all from the Department of Botany, Banaras Hindu University, India, following the method of Clemente et al. (2019). Rice samples were coded with 5 digits and consumers were asked to score the fumigated rice seeds using 1–5 hedonic scale. Analysis of results was based on the following patterns: 5 (like extremely), 4 (like moderately), 3 (neither like nor dislike), 2 (dislike moderately), and 1 (dislike extremely). The seeds were defined as unacceptable below the score of 2.

Phytotoxicity Assay of AGEO and Nm-AGEO-Fumigated Rice Seeds

Germination of rice seeds (fumigated and non-fumigated) were measured in terms of plumule and radicle emergence after 1 year of storage. For seed germination assay, Petri plates (9 cm) were moistened with double-layered blotting paper added with 1 mL of deionized water. Thereafter, four seeds were placed equidistantly in Petri plates and the emergence of radicle and plumule was observed at regular interval of 24–120 h.

Acute Toxicity Assay of AGEO and Nm-AGEO on Mice

Male mice (*Mus musculus* L., average weight 28.3 g and of 4 months old) were purchased from Institute of Medical Sciences, Banaras Hindu University, India, and acclimatized in laboratory conditions for 15 days. The study was performed after getting permission from Animal Care and Ethical Committee of the University. Required amounts (0.1–0.8 mL) of AGEO and Nm-AGEO were homogenized in 500 μL of aqueous Tween 20 (stock solution) to get desired concentrations and orally administered to mice through micropipette attached with catheter. The stock solution and negative control contained 500 μL Tween 20 and water, respectively. Effect of different doses was measured between 4 and 24 h and LD_{50} value was calculated by probit analysis.

Statistical Analysis

Experiments were done in three sets and data were represented in mean ± standard error format. Experimental data were analyzed through one-way analysis of variance (SPSS software, version 23, Chicago, IL, USA) at the significance level $P < 0.05$ with Tukey's multiple range tests.

Results and Discussion

Isolation and GC-MS of AGEO

Extracted AGEO was yellowish in color with spicy aroma and yield was 8 mL/kg of dry seeds. GC-MS analysis of AGEO showed 27 components representing 96.83% of essential oil. Table 1 depicts dill apiol (33.79%), carvone (27.19%), and limonene (13.76%) as the major components of AGEO. Similar finding on chemical composition of AGEO was reported by Kaur et al. (2019) but variation in percent composition of major components was found in this study. Yili et al. (2006) reported pentacosane (28%) and benzenedicarboxylic acid ester (25.1%) as the principal component of Chinese *Anethum graveolens* essential oil which could not be observed

Table 1 Chemical characterization (GC-MS) of AGEO

S No.	Retention time	Area (%)	Components	RI (Adams 2017)	Calculated RI
1	10.792	0.25	α-Thujene	930	1004
2	11.657	1.80	*P*-Cymene	1024	1026
3	11.969	13.76	**Limonene**	1029	1031
4	14.410	0.39	Fenchone	1086	1085
5	14.545	0.26	*P*-Cymenene	1091	1088
6	18.947	0.38	Dill ether	1186	1183
7	19.603	3.99	*Cis*-Dihydrocarvone	1192	1197
8	19.832	1.09	*Trans*-Dihydrocarvone	1200	1202
9	20.951	0.07	*Trans*-Carveol	1216	1227
10	22.054	27.19	**Carvone**	1243	1251
11	23.767	6.39	Anethole	1284	1289
12	24.470	0.19	Thymol	1290	1305
13	28.536	0.35	*Cis*-β-Guaiene	1493	1398
14	33.604	4.05	Myristicin	1518	1521
15	34.607	0.44	Elemicin	1557	1547
16	36.682	2.44	Carotol	1594	1600
17	38.057	33.79	**Dill apiole**	1620	1622
	Total	96.83			

Compounds in bold are major components

in our result. The variation may be due to climatic or altitudinal changes, different growth forms, inter-/intra-specific hybridization, and epigenetic modulations depending on habitat and varied distillation parameters. In addition, chemotypic variation, genetic backgrounds, and ploidy level significantly alter the transcriptome profile of genes controlling terpene synthesis, thereby causing effective alteration in sesquiterpenoids and phenolic components of essential oil (Bahmankar et al. 2019). Hence, GC-MS analysis is an important parameter to be considered while developing the plant-based formulation as green food preservative.

Preparation and Characterization of Nm-AGEO

Nanoencapsulation of essential oil is one of the effective technologies for improvement in stability as well as solubility of essential oil facilitating the development of subcellular nanoparticles with high carrying capacity, improved specificity, and controlled release with large surface area leading to enhancement in biological efficacy (Hemmatkhah et al. 2020). Ionic gelation is novel and convenient technique for the spontaneous synthesis of oil-in-water emulsion droplets with minimal utilization of surfactant and organic solvent and is completely based on the protonation as well as inter- and intra-molecular cross-linkage reactions in mild laboratory environmental conditions. In our study, chitosan was used as wall matrix for encapsulation of AGEO based on its versatile polymeric nature containing the unique features of biodegradability, biocompatibility, mucoadhesivity, high encapsulation efficiency, low toxicity, and controlled as well as targeted delivery actions (Hasani et al. 2018). The process of ionic gelation involves the incorporation of S-TPP as polyanionic cross-linker mediating electrostatic interaction between free amine groups of chitosan during the high-pressure homogenization resulting into polyelectrolyte complexes with efficient entrapment of AGEO within chitosan matrix. Different ratio of chitosan to AGEO (w/v) (1:0, 1:0.2, 1:0.4, 1:0.6, 1:0.8, and 1:1) was prepared to determine maximum imprisoning of AGEO within chitosan nanobiopolymer. Furthermore, the inclusion of chitosan and S-TPP under GRAS category strengthens the future exploitation of AGEO loaded chitosan nanoemulsion for extension of shelf-life of stored food products in food and agricultural industries (Singh et al. 2019; Ahmadi et al. 2018).

SEM Investigation

Surface morphology (texture as well as surface roughness) of chitosan nanoparticle and Nm-AGEO nanoparticle was determined through SEM analysis. Figure 1a, b represents the SEM of chitosan nanoparticle and Nm-AGEO nanoparticle exhibiting irregular structures with certain degree of aggregations. Spherical shapes of chitosan nanoparticle and Nm-AGEO nanoparticles were observed only at some places. Reduced numbers of spherical nanoparticles were found at some places while aggregation was observed at majority of the portions probably due to particle interaction together with combining and melting effects of lyophilization. Some

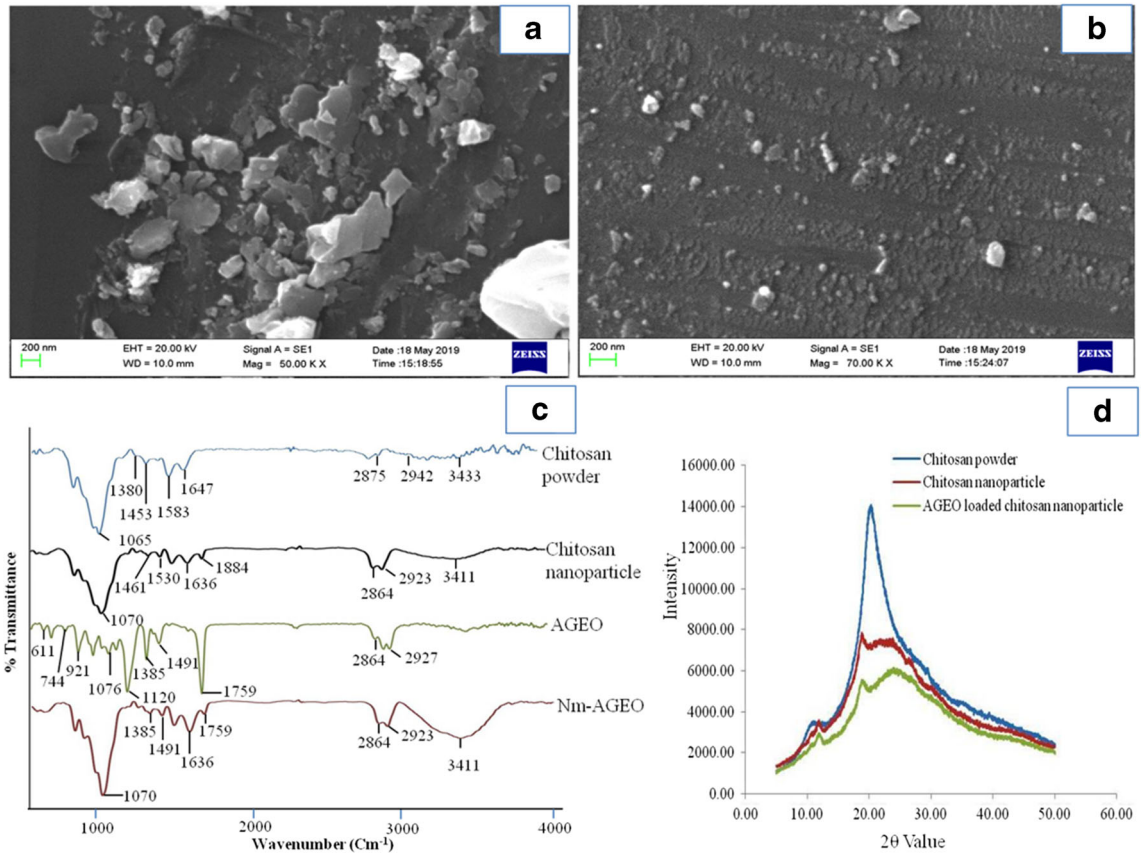

Fig. 1 SEM image of chitosan nanoparticle (**a**); SEM image of AGEO-loaded chitosan nanoparticle (Nm-AGEO) (**b**); FT-IR spectra of chitosan, chitosan nanoparticle, AGEO, and Nm-AGEO nanoparticle (**c**); and XRD diffraction pattern of chitosan, chitosan nanoparticle and Nm-AGEO nanoparticle (**d**)

spherical shapes of nanoparticles may be due to the utilization of 0.4% S-TPP solution causing complete inter and intramolecular cross-linking (Woranuch and Yoksan 2013). However, the roughness observed on the surface of the irregular structures could be due to characteristic lyophilization via formation of cracks, ruptures, and fissures with somewhat particle aggregation. It was critically observed that Nm-AGEO nanoparticles (Fig. 1b) were smaller in size than chitosan nanoparticles (Fig. 1a). The particle size determined by dynamic light scattering ranged from 62 to 86 nm. Incorporation of AGEO led to somewhat reduction in size of Nm-AGEO nanoparticle and also facilitated the homogeneous distribution. Dwivedy et al. (2018) have also observed the same trend in reduction of droplet size (below 200 nm) of *Illicium verum* essential oil after effective encapsulation into chitosan nanomatrix; however, our finding demonstrated much smaller particle size after entrapment of AGEO within chitosan nanobiopolymer indicating the suitability of the fabricated nanoparticle for effective protection against stored food biodeterioration by interacting at the surfaces and interfaces where fungal cells easily proliferate and secrete aflatoxins. Our result is consistent with previous investigation of Da Silva Gündel et al. (2018) showing prominent interaction with *Cymbopogon flexuosus* essential oil and polycationic wall material as well as involvement of Tween 80 causing effective compaction and stabilization leading to reduced size of nanoparticle with efficient inhibitory action against food pathogenic bacteria.

FT-IR Investigation

Figure 1c represents FT-IR spectra of chitosan, chitosan nanoparticle, AGEO, and Nm-AGEO nanoparticle. Chitosan showed different peaks at 1065 (C–O stretching), 1380 (–OH bending vibration), 1453 (–CH stretching aromatic ring), 1583 (–NH bending secondary amine), 1647 (amide I), 2875, 2942 (asymmetric and symmetric $–CH_2$ stretching vibrations), and 3433 cm^{-1} ($–NH_2$ and –OH stretching). Chitosan nanoparticle displayed shifting of peak from 1065 to 1070 cm^{-1}, 2875 to 2864 cm^{-1}, and 2942 to 2923 cm^{-1}. Moreover, the peak at 1070 cm^{-1} as represented by P=O stretching from phosphate groups indicated the formation of nanoparticle complex through electrostatic interaction between chitosan and S-TPP by ionic gelation. Shifting of peak from 1583 to 1530 cm^{-1} also confirmed the intermolecular interaction between chitosan and S-TPP (Shah et al. 2016). Further, the

chitosan S-TPP interaction was also observed from wave number 891 to 3411 cm^{-1} based on peak displacements, broadening, shifting, stretching, bending, and vibrations. Pure AGEO showed characteristic peaks at 611 (pyranoside ring stretching), 744 (–CH bending), 921 (P=O bending), 1076, 1120 (–C–O–C stretching), 1451 (C=C bending), 2864 (–CH stretching at methylene hydrogen), and 2927 (–CH stretching) cm^{-1} (Shetta et al. 2019) illustrating the presence of different constituents of essential oil. Interestingly, after encapsulation of AGEO within chitosan nanoparticle, most of the characteristic peaks of chitosan nanoparticle and AGEO appeared in Nm-AGEO nanoparticle with minor changes in the wave number and stretching vibrations indicating a possible chemical interaction between AGEO and chitosan nanoparticle.

XRD Analysis

XRD analysis of chitosan, chitosan nanoparticle, and Nm-AGEO nanoparticle showed different diffraction patterns (Fig. 1d). Chitosan exhibited two different crystal peaks viz form I (11.0°) and form II (21.5°) representing high degree of crystallinity. Cross-linking of PO_4^{3-} groups of S-TPP with NH_3^+ groups of chitosan led to broadening as well as shifting of peak intensity in the chitosan nanoparticle indicating destruction of native crystallinity of chitosan powder (Amalraj et al. 2020). Entrapment of AGEO within chitosan matrix led to much broadened peak intensity representing the further increase in amorphous nature of Nm-AGEO nanoparticle, thereby suggesting alteration in chitosan–TPP packing behavior and effective changes in hydrogen bonding pattern (Rajkumar et al. 2020). Hence, differences in XRD patterns confirmed the successful encapsulation of AGEO because of electrostatic interaction between chitosan, TPP, and active components of AGEO. Destruction in crystallinity of native chitosan powder after incorporation of AGEO droplets offers its greater stability for active tight packaging of volatile components and reinforces the compatibility of AGEO-loaded chitosan nanoparticle for practical application in food system.

Encapsulation Efficiency, Loading Capacity, and Nanoparticle Yield of Nm-AGEO

Table 2 represents percent EE, LC, and NY of Nm-AGEO as measured through spectrophotometric determination at 285 nm. EE % ranged from 17.84 to 85.51%. Initial increment of EE up to ratio 1:0.8 (w/v), followed by decreasing pattern was observed for different ratio (w/v) of chitosan to AGEO. Entrapment of AGEO into chitosan matrix depends on several parameters such as property and concentration of surfactant used, different functional groups of AGEO, and variable environmental factors viz temperature and pH. Decreasing pattern of EE at higher chitosan to AGEO ratio (1:1) may be explained as less efficient dispersive forces during homogenization resulting into coalescence of the oil globules with decrement in wall thickness of nanoemulsion system and insufficient amount of polymer chitosan for complete encapsulation of AGEO (Hussain and Maji 2008). The loss of larger oil vesicles during centrifugation and saturation of AGEO at higher loading concentrations may be another reason for decrement of EE and LC (Hosseini et al. 2013). LC % of different chitosan to AGEO ratio (w/v) ranged from 1.08 to 4.05%. LC values exhibited similar trend as maximum EE and LC was found at 1:0.8 (w/v) ratio. Our result is in accordance with Jiang et al. (2020) suggesting decrement in encapsulation efficiency and loading capacity of lemon essential oil-loaded chitosan nanoparticle after a certain limit due to saturation of essential oil in nanoparticle-embedded chitosan matrix. Previous investigation of Ghaderi-Ghahfarokhi et al. (2016) suggested maximum capacity for efficient entrapment and loading of Thyme essential oil into chitosan nanomatrix as 30.67 and 13.71%, respectively. In another study of Feyzioglu and Tornuk (2016), maximum encapsulation efficiency of summer savory essential oil loaded into chitosan nanoparticle was found to be 40.70%. However, our finding illustrated better performance in entrapment of AGEO into chitosan biopolymer up to 85.51% which promptly supports the superiority of the wall material to maximally protect the AGEO degradation under the fluctuating environmental conditions. Nanoparticle yield of Nm-AGEO at 1:0.8 (w/v) ratio (maximum entrapment of AGEO) was found to be 28.36%. Higher nanoparticle yield suggests the efficient entrapment of AGEO droplets into chitosan matrix with maximum stability. Similar result of encapsulation yield has been recently demonstrated by Hasheminejad et al. (2019) for encapsulation of clove essential oil in chitosan nanoparticle. Hence, the present investigation suggests the desirable property of Nm-AGEO to maximize its application as food preservative by efficient entrapment and imprisoning of volatile constituents in order to inhibit the fungal and aflatoxin contamination and extend the maximum product shelf-life.

Release Tests of Nm-AGEO

Figure 2a depicts the biphasic cumulative release of AGEO from chitosan nanoemulsion in PBS at 285 nm. Our investigation revealed the biphasic release behavior of AGEO from chitosan nanomatrix confirming its controlled volatilization and suggests the suitability of wall matrix as a prominent barrier around AGEO throughout the storage and pH susceptibility of encapsulated AGEO which is an important factor for further exploitation of Nm-AGEO as smart delivery vehicle for eco-friendly preservation of stored food commodities. About 21.01% of AGEO was released within first 4 h followed by 17.37 and 12.08% release between (4–8 h) and (8–12 h). In the second phase of incubation (20–24 h), the rate of

Table 2 Encapsulation efficiency (EE), loading capacity (LC), and nanoparticle yield (NY) of Nm-AGEO

Chitosan/AGEO (w/v)	Encapsulation efficiency (%)	Loading capacity (%)	Nanoparticle yield (%)
1:0	0.00 ± 0.00^{a}	0.00 ± 0.00^{a}	–
1:0.2	17.84 ± 2.86^{b}	1.08 ± 0.07^{b}	–
1:0.4	31.91 ± 2.90^{c}	1.94 ± 0.13^{c}	–
1:0.6	61.23 ± 3.78^{d}	3.31 ± 0.10^{c}	–
1:0.8	85.51 ± 3.05^{d}	4.05 ± 0.11^{d}	28.36 ± 1.69
1:1	54.68 ± 3.09^{e}	2.09 ± 0.08^{e}	–

Values are mean (n = 3) ± SE; the means followed by the same letter in the same column are not significantly different according to ANOVA and Tukey's multiple comparison tests

– not determined

cumulative release was 5.62%. After 72 h of incubation, the release rate (2.41%) was comparatively lower indicating a biphasic burst. Motwani et al. (2008) explained the initial burst release of essential oil due to significant hydrophilicity of chitosan leading to rapid hydration of particle in nanoemulsion system. Large amount of AGEO on the surface of the polymer matrix forming weak linkage could be considered as an important factor for initial burst release. Decrement in AGEO release with respect to time may be due to reduced diffusion and concentration gradients between Nm-AGEO dissolved in PBS solution as well as inability of buffer solution to break compact form of particle in nanoemulsion system (Agnihotri et al. 2004). Similar finding on biphasic release profile of cumin essential oil from chitosan nanoparticle has been recently observed (Amiri et al. 2020). They suggested initial burst release of cumin essential oil in the first 5 h followed by later sustained release within 24–48 h. Karam et al. (2020) demonstrated the significant release (2–8%) of *Matricaria chamomilla* essential oil from chitosan nanocapsules within very short periods of time (0–72 h). However, our finding exhibited superiority in biphasic release kinetics and controlled volatilization of chitosan entrapped AGEO up to a period of 24–150 h. The sustained release profile of AGEO for long-term duration implies the suitability of our investigated process and selection of chitosan biopolymer as a good alternative for encapsulation of volatile AGEO, thereby affirming the stability of Nm-AGEO as well as controlled release of volatile components resulting in long-term efficacy for inhibition of fungal infestation and AFB_1 contamination in stored food products.

In Vitro Antifungal and Antiaflatoxigenic Efficacy of AGEO and Nm-AGEO

Antifungal efficacy of AGEO and Nm-AGEO was evaluated for the first time on the basis of comparative assessment for inhibition of AF LHP R14 cells. AGEO completely inhibited growth of AF LHP R14 strain (represented as mycelial dry weight (MDW)) at 1.2 μL/mL, while better antifungal efficacy was exhibited by Nm-AGEO at 0.6 μL/mL (Table 3). AGEO showed far better fungitoxic results than previously reported sulfur fungicides, BHT, and some essential oils viz *Myristica fragrans* (Das et al. 2020a) and *Luvunga scandens* (Dubey et al. 2017). Both the AGEO and Nm-AGEO showed broad-range fungitoxicity against common food biodeteriorating molds (Fig. 2b). In addition, AGEO and Nm-AGEO significantly checked AFB_1 secretion by AF LHP R14 strain at 0.8 and 0.4 μL/mL, respectively (Table 3). No considerable inhibition of AF LHP R14 cell growth and AFB_1 secretion was exhibited by chitosan nanoemulsion (data not shown) that might be due to utilization of all free amine and hydroxyl groups during encapsulation. Interestingly, the lower dose antifungal and antiaflatoxigenic activity of Nm-AGEO may suggest the novel synergistic actions of AGEO with chitosan nanomatrix facilitating better reaction kinetics and revealed good inter-connective and appropriate interactions (Amjadi et al. 2019; Das et al. 2021b) with excellent compatibility for practical utilization in food and agricultural industries. Previous investigation of Kalagatur et al. (2018) reported effective inhibition of pathogenic fungi such as *Fusarium graminearum* and their associated toxins in maize grains viz zearalenone and deoxynivalenol by *Cymbopogon martinii* essential oil incorporated into chitosan nanocapsules; however, our result suggested superior efficacy in inhibition of broad-spectrum food-contaminating fungi including the toxigenic species of *A. flavus* (AF LHP R14) and AFB_1 secretion after entrapment of AGEO into chitosan nanoemulsion. Moreover, better diminution potentiality of Nm-AGEO against AFB_1 secretion may be due to downregulation of some key enzymes of carbohydrate catabolism that induce AFB_1 biosynthesis, reduction of fungal sporulation, and controlled release of volatile components of AGEO as well as nano size of AGEO droplets that may enhance the site specific efficacy of Nm-AGEO on the food interfaces (López-Meneses et al. 2018).

Both, AGEO and Nm-AGEO caused significant inhibition of spore germination. At the MIC concentration of AGEO, inhibition of spore germination was found to be 79.33%,

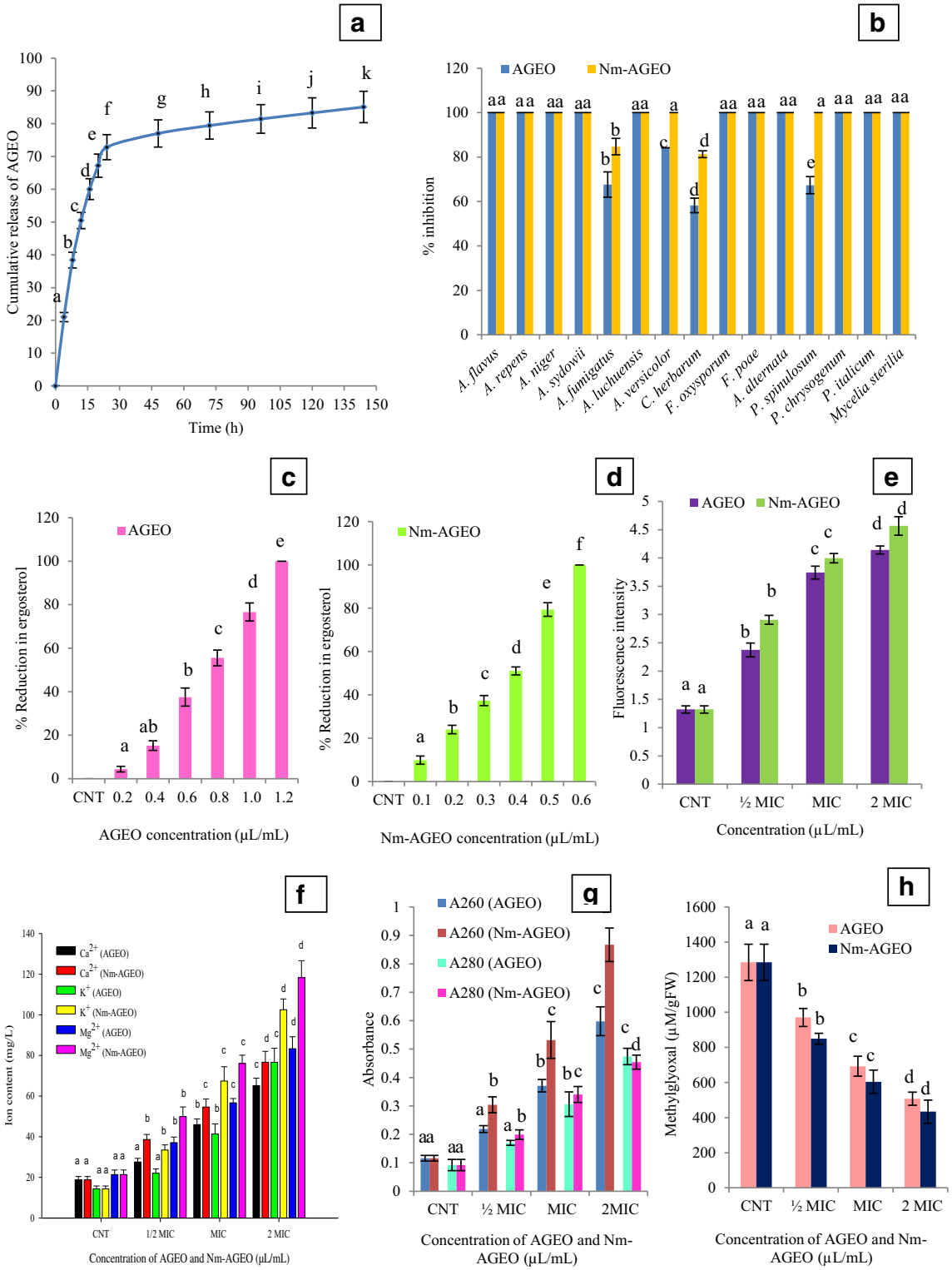

Fig. 2 In vitro release behavior of Nm-AGEO (**a**), fungitoxic spectrum of AGEO and Nm-AGEO against common food deteriorating molds (**b**), effect of AGEO on cellular ergosterol (**c**), effect of Nm-AGEO on cellular ergosterol (**d**), effect of AGEO and Nm-AGEO on membrane integrity by PI fluorescence intensity assay (**e**), effect of AGEO and Nm-AGEO on efflux of cellular ions (Ca^{2+}, K^{+}, Mg^{2+}) (**f**), effect of AGEO and Nm-AGEO on leakage of A_{260} and A_{280} nm absorbing materials (**g**), and effect of AGEO and Nm-AGEO on methylglyoxal biosynthesis (**h**)

Table 3 Effect of AGEO and Nm-AGEO on mycelial dry weight (MDW) and AFB_1 inhibition

AGEO			Nm-AGEO		
Conc. (μL/mL)	MDW (g)	% inhibition of AFB_1	Conc. (μL/mL)	MDW (g)	% inhibition of AFB_1
CNT	1.08 ± 0.07^{a}	0.00 ± 0.00^{a}	CNT	1.08 ± 0.07^{a}	0.00 ± 0.00^{a}
0.2	0.84 ± 0.02^{b}	18.05 ± 4.80^{b}	0.1	0.79 ± 0.03^{b}	27.73 ± 3.25^{b}
0.4	0.69 ± 0.04^{c}	58.26 ± 5.76^{c}	0.2	0.60 ± 0.02^{c}	53.40 ± 4.95^{c}
0.6	0.45 ± 0.03^{d}	84.37 ± 4.99^{d}	0.3	0.45 ± 0.03^{d}	87.33 ± 3.04^{d}
0.8	0.26 ± 0.03^{e}	100 ± 0.00^{e}	0.4	0.30 ± 0.02^{e}	100 ± 0.00^{e}
1.0	0.15 ± 0.02^{e}	–	0.5	0.06 ± 0.03^{f}	–
1.2	0.00 ± 0.00^{f}	–	0.6	0.00 ± 0.00^{f}	–

Values are mean ($n = 3$) ± SE; the means followed by the same letter in the same column are not significantly different according to ANOVA and Tukey's multiple comparison tests

MDW mycelial dry weight, *CNT* control, – not determined

while Nm-AGEO exhibited 97.43% inhibition at its MIC dose. Our result corroborated with the recent finding of Dammak et al. (2019) showing mycosporicidal activity of *Lavandula dentata*, *Salvia officinalis*, and *Laurus nobilis* essential oils. Inhibition of sporulation by AGEO and Nm-AGEO fumigation may be a possible reason for significant reduction in AFB_1 biosynthesis.

Biochemical Mechanism of Action of AGEO and Nm-AGEO Against AF LHP R14 Cells and AFB_1 Secretion

Ergosterol is an important fungal sterol maintaining membrane fluidity, permeability, as well as biogenesis and transcription of specific ligands and receptors available for membrane bound enzymes (Yang et al. 2015). Ergosterol has been suggested as marker determinant for fungal and mycotoxin contamination in agricultural commodities during long-term storage (Porep et al. 2015). Hence, the investigation on the effect of AGEO and Nm-AGEO on cellular ergosterol biosynthesis has been determined for the first time. AF LHP R14 cells fumigated with AGEO at concentrations 0.2, 0.4, 0.6, 0.8, 1.0, and 1.2 μL/mL caused 4.40, 15.18, 37.52, 55.54, 76.72, and 100% reduction of ergosterol content, respectively, while Nm-AGEO showed better efficacy in ergosterol reduction at lower doses (Fig. 2c, d). Chitosan nanoemulsion did not exhibit any considerable effect on ergosterol retardation (data not shown). Impairment in ergosterol biosynthesis in all the treated sets may be due to disruption of key enzyme (lanosterol 14 α-demethylase) in ergosterol biosynthesis as well as destabilization of plasma membrane as earlier reported for azole groups of antifungal agents (Pinto et al. 2006). Superior performance of Nm-AGEO on inhibition of ergosterol biosynthesis was resulted due to synergistic interactions of AGEO with chitosan nanomatrix and binding of nano sized AGEO droplets (greater surface area to volume ratio) with membrane ergosterol altering the physical state of plasma membrane leading to rapid depletion of membrane integrity (Radhakrishnan et al. 2018). Singh et al. (2019) suggested significant impairment in ergsoterol biosynthesis by higher concentrations of *Ocimum sanctum* essential oil-loaded chitosan nanoemulsion; however, our finding demonstrated better performance in terms of ergosterol inhibition at comparatively lower doses than the previous investigation that might be due to small sized AGEO nanocapsules with better target site delivery and controlled release. Hence, the present investigation illustrates a new insight for the development of natural antifungal food preservative via effectively restricting the synthesis of ergosterol.

Propidium iodide is an important fluorescent nucleic acid binding dye acting as viability marker of cells that cannot pass through the intact plasma membrane of viable cells. All the fumigated sets caused increased fluorescent intensity at MIC and 2 MIC concentrations after 30 min of incubation (Fig. 2e). Increasing fluorescent intensity with respect to different doses of AGEO and Nm-AGEO suggested the formation of membrane lesions and destruction of membrane integrity as well as stability, thereby causing intercalation of propidium iodide in the nuclei and binding with DNA double helix (Choi et al. 2013).

Moreover, all the fumigated AF LHP R14 cells showed significant efflux of Ca^{2+}, K^{+}, and Mg^{2+} ions as well as major cytoplasmic materials (260 and 280 nm absorbing elements) in extracellular medium with respect to different doses (Fig. 2f, g). This may be due to hydrophobic interaction of AGEO and Nm-AGEO with plasma membrane, crossing the barrier and disturbing the fluidity by altering membrane lipid leading to enhanced leakage of cellular metabolites and considerable changes in internal homeostasis of different cellular organelles which actively participate in AFB_1 synthesis (Shao et al. 2013). Our present result indicated that Nm-AGEO treatment effectively destabilized the membrane integrity and permeability by efflux of vital cellular ions and cytoplasmic constituents, thereby suppressing the fungal infestation resulting in mitigation of aflatoxin contamination and prolonged preservation periods.

Methylglyoxal (MG) (α, β-dicarbonyl aldehyde) is a potent glycating molecule forming different glycation adducts with cysteine, arginine, and lysine residues of proteins and nucleic acids, thus altering cellular metabolism. MG is reported to induce the synthesis of aflatoxins in food products and enhance the production of ROS through impairment of glutathione level (Das et al. 2019). Therefore, in this study the impact of AGEO and Nm-AGEO on cellular MG biosynthesis has been carried out for the first time. Higher level (1284.60 μM/gFW) of MG was found in control set, while samples treated with AGEO and Nm-AGEO exhibited significant reduction in MG content at MIC (692.70 and 604.36 μM/gFW) and 2 MIC (508 and 433.99 μM/gFW) concentrations (Fig. 2h). Considerable reduction in MG level may be correlated with dose-dependent AFB_1 reduction by downregulating constitutive expression of afl-R and nor-1 gene products (Upadhyay et al. 2018). Superior performance of Nm-AGEO on inhibition of cellular MG may be ascribed to better antioxidant profile and synergistic actions of AGEO after encapsulation into chitosan nanomatrix. Thus, the present study strengthens the application of Nm-AGEO as smart delivery vehicle for preservation of stored food commodities via mitigation of MG level and suggests a new horizon for development of aflatoxin-resistant varieties through sustainable green transgenic technology.

In Silico Molecular Docking of Carvone and Limonene with AFB_1 Biosynthetic Regulatory Gene *Omt-A* and *Ver-1*

Remarkable in vitro antifungal and antiaflatoxigenic activity as reveled through biochemical mechanism of action of AGEO and Nm-AGEO prompted us to have an understanding about molecular mechanism of AFB_1 inhibition using in silico approaches. Hence, in our investigation, two key regulatory genes viz *Ver-1* and *Omt-A* were selected based on their active participation in conversion of versicolorin A to sterigmatocystin and sterigmatocystin to *O*-methylsterigmatocystin, respectively. Three-dimensional (3D) structure of ver-1 protein was modeled with dimension of *X*: 49.430, *Y*: 57.759, and *Z*: 46.324. All the 262 amino acid residues were in the range of 90% confidence. 3D structure of Omt-A was modeled with dimension of *X*: 62.644, *Y*: 53.797, and *Z*: 67.304 with more than 90% of confidence. FIRE-DOCK online tool was utilized for the selection of the best protein-ligand interacting model based on global energy, attractive van der Waals force (VdW), repulsive van der Waals force (VdW), and atomic contact energy (ACE) (Table 4). Different parameters of energy indices provided significant information about the molecular target site determination by in silico studies (Usha et al. 2014). Carvone and limonene interacted with Ala 95, Gly 136, Thr 15, Arg 19, and Asp 194 amino acids residues of Ver-1, while Gln 358, Leu 38, Arg 359, Glu 34, and Hsd 36 interacted with Omt-A protein (Fig. 3a–f). Our findings showed observations similar to Murugan et al. (2013), Badawy et al. (2019), and Das et al. (2020b) suggesting potential molecular interaction of the components with enzymatic transcripts for inside penetration leading to conformational impairment in hydrogen bonding-dependent stereo-spatial shapes of the catalytic portion that could be a prime reason for AFB_1 inhibition.

Effect of AGEO and Nm-AGEO on Enzymatic and Non-enzymatic Defense System of AF LHP R14 Cells

Different enzymatic (SOD, CAT) and non-enzymatic (GSH/GSSG) defense biomolecules play key catalytic role in alleviation of cellular oxidative stress and demonstrate a novel biochemical mechanism of action for inhibition of fungal growth and AFB_1 secretion. Therefore, the effect of AGEO and Nm-AGEO on different antioxidative defense markers viz ROS, SOD, CAT, and glutathione (GSH/GSSG) in AF LHP R14 cells was determined for the first time in our present investigation. All the fumigated sets at ½ MIC and MIC doses with AGEO and Nm-AGEO exhibited significant increment in ROS production as compared to control (Fig. 4a). Mitochondria are the major site of ROS generation in eukaryotic cells. Although ROS actively participate in cell viability, excessive ROS production under oxidative stress may effectively depolarize the mitochondrial membrane potential, inactivate enzymatic activities, and disrupt normal functioning of major cellular organelles causing alteration in biochemical profile. DCFH-DA is a non-fluorescent dye, but after crossing the plasma membrane barrier, it is converted into fluorescent DCF by the activity of cellular esterase. The amount of DCF formed can be measured directly to determine the increment in ROS level. Induced ROS production may cause alteration in chromatin remodeling, phosphatidylserine externalization, and ultimately cell death by apoptosis (Kong et al. 2019). To compensate the oxidative stress, battery of cellular antioxidative enzymes (SOD and CAT) is involved with significant reduction of free radical load. SOD transforms different peroxides and superoxide radicals into H_2O_2, while CAT participates in conversion of H_2O_2 to H_2O and oxygen (Weydert and Cullen 2010). In control set, CAT and SOD levels were 9.62 and 14.4 unit/mg protein, respectively, while in AGEO and Nm-AGEO fumigation at ½ MIC and MIC dose, the levels of CAT and SOD were determined as 5.2, 24.53, and 2.88, 31.12 unit/mg protein, respectively (Fig. 4b, c). Previous investigation of Kou et al. (2014) and Molamohammadi et al. (2020) suggested the effect of chitosan coating on concentration-dependent increment in cellular SOD and CAT activity; however, our result contradicted from the previously published reports and demonstrated two different patterns viz concentration-dependent (a) decrement in cellular CAT and (b) increment in cellular SOD level, suggesting a novel biochemical mechanism involved in mitigation of cellular

Table 4 Energy indices parameter for effective molecular interaction of carvone and limonene with Ver-1 and Omt-A proteins

Receptor	Ligands	Hydrogen bonding with amino acids	Energy indices (kcal/mol)			
			Global energy	Attractive van der Waals	Repulsive van der Waals	Atomic contact energy
Ver-1	Carvone	Ala 95, Gly 136, Thr 15	− 27.33	− 12.01	0.98	− 6.83
	Limonene	Arg 19, Asp 194	− 27.19	− 11.94	0.88	− 7.44
Omt-A	Carvone	Gln 358, Leu 38, Arg 359	− 28.67	− 11.23	1.25	− 8.13
	Limonene	Gln 358, Glu 34, Hsd 36	− 26.09	− 10.19	0.19	− 7.13

oxidative stress. Moreover, variable changes in the level of intracellular SOD and CAT may inhibit the AFB_1 biosynthesis through modulation of bZIP transcription factors (ap-1, atf A, and atf B) as well as regulated expression of aflatoxin regulatory genes viz *cat*2, mn *SOD*, *afl D*, *afl T*, and *afl M* in peroxisomes and aflatoxisomes (Lv et al. 2018). It has been reported that aflatoxins are mainly biosynthesized in peroxisomes and aflatoxicosomes having significant association with SOD and CAT-synthesizing genes. Hence, Nm-AGEO-mediated modulation of different transcription factors associated with antioxidative defense enzymes triggered cope up mechanism for alleviating cellular oxidative stress, a prerequisite condition for mitigation of AFB_1 biosynthesis (Sun et al. 2016; Grintzalis et al. 2014; Adisa et al. 2019). In addition to cellular CAT and

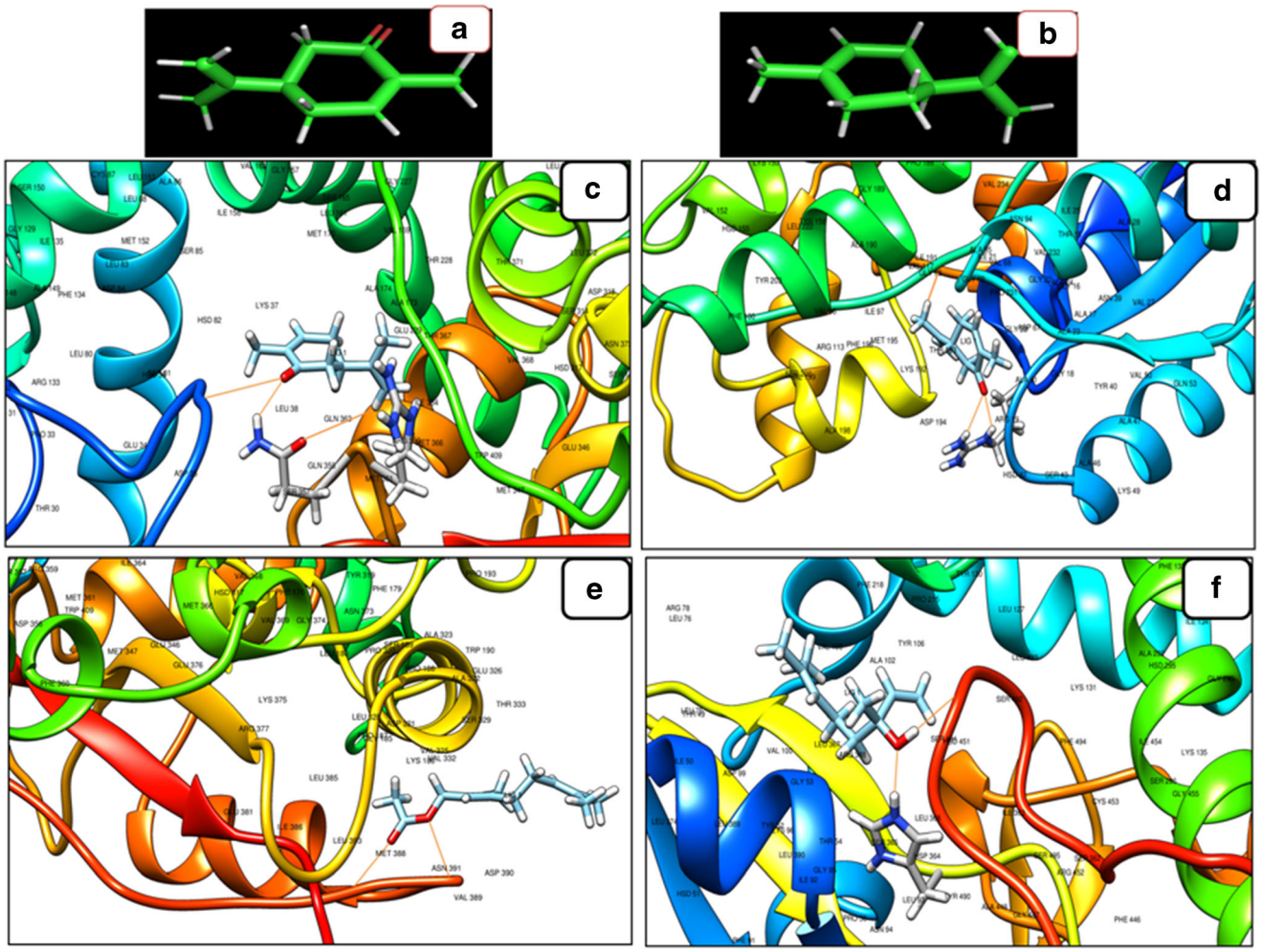

Fig. 3 Three-dimensional (3D) structures of carvone (**a**) and limonene (**b**), in silico molecular interaction between Ver-1 and carvone (**c**), Ver-1 and limonene (**d**), Omt-A and carvone (**e**), and Omt-A and limonene (**f**)

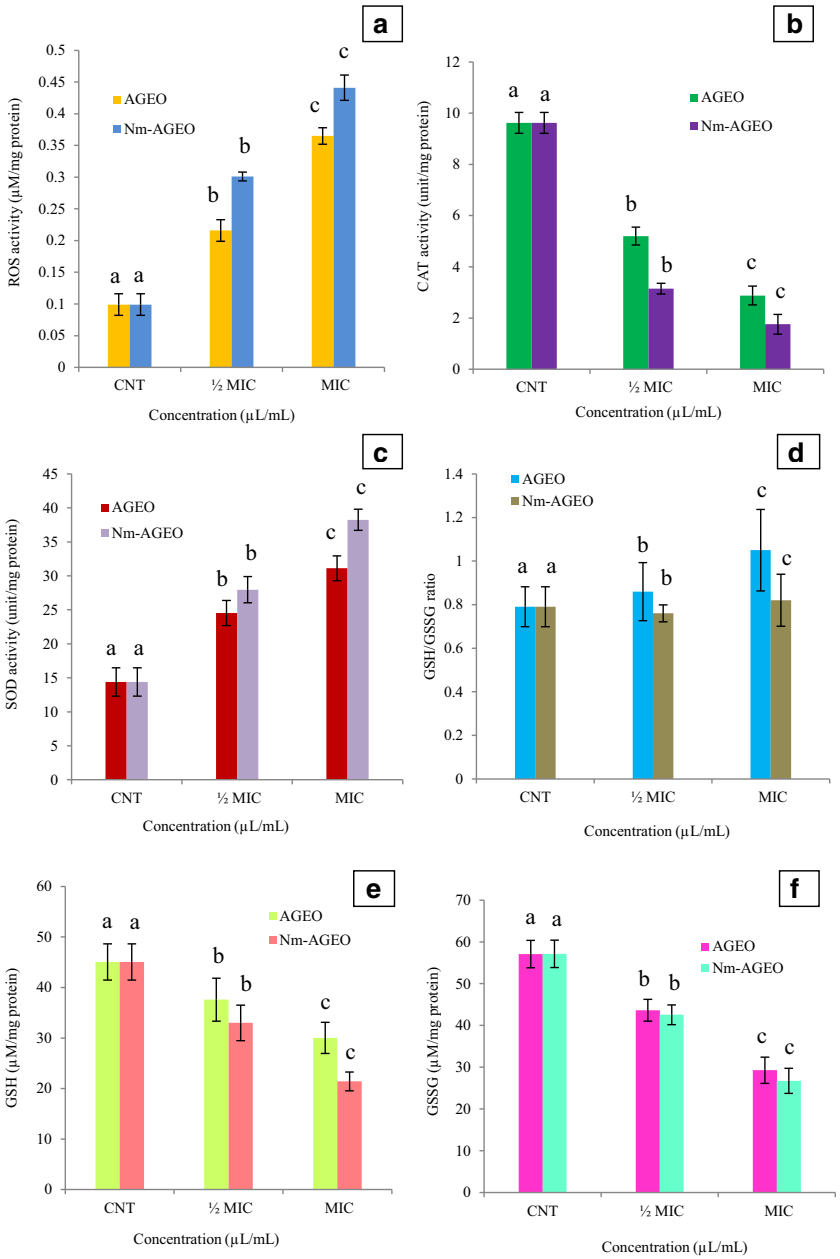

Fig. 4 Effect of AGEO and Nm-AGEO on ROS (**a**), CAT (**b**), SOD (**c**), GSH/GSSG ratio (**d**), GSH (**e**), and GSSG (**f**)

SOD levels, AGEO and Nm-AGEO caused enhancement in the level of GSH/GSSG ratio and decreased synthesis of GSH and GSSG (Fig. 4d–f). Chitosan nanoemulsion did not exhibit any significant effect on CAT, SOD, and GSH/GSSG activity (data not shown). GSH is one of the important non-enzymatic biomolecules acting as intracellular buffer for amelioration of oxidative stress by reducing the hydro-peroxides radicals (ROOH) and xenobiotic toxicity. Hence, modulation in enzymatic and non-enzymatic antioxidant defense biomolecules demonstrates a new horizon to maximize the practical application of Nm-AGEO as next-generation smart green preservative with emphasis on antioxidant defense system-based mitigation of fungal infestation and AFB_1 contamination in stored food commodities.

Total Phenolic Content and In Vitro Radical Scavenging Activity of AGEO and Nm-AGEO

Instead of fungal and AFB_1 contamination, oxidative stress in stored food products is also directly involved in biodeterioration process. Therefore, determination of phenolic content and antioxidant activity of essential oil and its nanoformulation is of prime importance for their efficient practical applicability as green preservative. Total phenolic content of AGEO was found to be 9.41 mg/gallic acid equivalent, while encapsulation of AGEO into chitosan nanomatrix effectively reinforced the phenolic content up to 13.80 mg gallic acid equivalent. Chitosan nanoemulsion showed very low phenolic content (1.24 mg gallic acid equivalent) that might be explained

through reaction kinetics of non-phenolic components with Folin–Ciocalteu's reagent leading to development of less amount of colored chromogens (Ruiz-Navajas et al. 2013). Our result is consistent with previous investigation of Zheng et al. (2017) exhibiting augmenting effect of chitosan coating on phenolic content of kiwifruit. The antioxidant activity of AGEO and Nm-AGEO was determined through DPPH$^{\cdot}$ and ABTS$^{\cdot+}$ assay. IC_{50} values of AGEO were found to be 8.62 and 4.23 μL/mL for DPPH$^{\cdot}$ and ABTS$^{\cdot+}$ assay, respectively, while encapsulation of AGEO within chitosan nanomatrix exhibited superior antioxidant activity ($IC_{50\ DPPH}$ = 4.30 and $IC_{50\ ABTS}$ = 2.49 μL/mL). Chitosan nanoemulsion exhibited negligible antioxidant potency that may be due to the masking of free amine groups through efficient cross-linking with S-TPP which is described to actively participate in reaction with DPPH$^{\cdot}$ and ABTS$^{\cdot+}$ radical (Shetta et al. 2019). Significant radical scavenging potency of AGEO may be due to the presence of major terpenoid components such as carvone, limonene, and camphor as well as some phenolic components along with their synergistic action (Kaur et al. 2019). Enhancement in free radical scavenging activity of Nm-AGEO could be resulted due to controlled release of AGEO from chitosan nanomatrix having greater surface to volume ratio with effective absorption of DPPH$^{\cdot}$ and ABTS$^{\cdot+}$ molecules in the emulsion system (Sharifimehr et al. 2019). Improvement in antioxidant activity of clove essential oil incorporated into chitosan nanoparticle has been recently demonstrated by Hadidi et al. (2020). Significant hydrogen bonding interaction of hydroxyl groups present in phenolic components with polycationic wall matrix causing sustained release of extract could be suggested as a possible mechanism for enhancement in antioxidant activity. Wang et al. (2017) suggested effective reinforcement in antioxidant activity of cinnamon and ginger essential oil after encapsulation into chitosan biopolymer. They suggested prominent oxygen barrier potentiality of chitosan matrix responsible for improvement in antioxidant activity. However, our finding demonstrated superior antioxidant efficacy of Nm-AGEO than the previous investigations suggesting novel natural substitute for elimination of harmful effects of synthetic antioxidants and application of encapsulated essential oil as smart delivery vehicle for controlling the fungal and aflatoxin contamination mediated biodeterioration of stored food commodities.

In Situ Preservative Efficacy of AGEO and Nm-AGEO Against Fungal Infestation, AFB_1 Secretion, and Lipid Peroxidation in Stored Rice (the Model Food System)

In the in vitro investigation, both the AGEO and Nm-AGEO, displayed remarkable efficacy for inhibition of fungal growth and AFB_1 secretion; hence, the further evaluation of AGEO and Nm-AGEO as ideal preservative fumigant in food system was necessary to support the notion of better suitability for their practical application. Therefore, rice was selected as model food system to demonstrate the effect of AGEO and Nm-AGEO against fungal infestation, AFB_1 secretion, and lipid peroxidation during storage. In situ experiments containing model food system is a major parameter of the study as biological efficacy of essential oils and their nanoformulation is diversely regulated in the food system based on the moisture, pH, relative humidity, temperature and chemical constituents of the food commodities. Figure 5a–j represents the control as well as AGEO and Nm-AGEO-treated rice samples at respective MIC and 2 MIC doses. Percent inhibition of *A. flavus* contamination in AGEO and Nm-AGEO-fumigated rice seeds at the MIC and 2 MIC concentrations (inoculated + uninoculated treatments) were found as 57.65, 71.23 and 61.23, 82.11%, respectively (Fig. 6a). Inoculated and uninoculated control sets represented higher level of AFB_1 as determined through HPLC analysis viz, 29.57 and 25.01 μg/kg, respectively. However, complete inhibition of AFB_1 secretion was exhibited by both the AGEO and Nm-AGEO at both MIC and 2 MIC-fumigated sets. Interestingly, 100% inhibition of *A. flavus* contamination was not found in both AGEO and Nm-AGEO-fumigated rice seeds that might be due to absorption/adsorption of some of the volatile components by food commodity itself. Complete inhibition of AFB_1 contamination in AGEO and Nm-AGEO-fumigated sets may suggest differential mechanism of action inhibiting carbohydrate catabolism based on energy mediated toxin generation (Das et al. 2019). The in vitro mitigation of cellular methylglyoxal (AFB_1 inducer) supports the notion of better antiaflatoxigenic efficacy of AGEO and Nm-AGEO for protection of rice seeds against AFB_1 secretion during storage. Moreover, the encapsulated AGEO showed much better antifungal and antiaflatoxigenic efficacy for preservation of food commodities than some commonly used organic preservatives such as formic acid, propionic acid, benzoic acid, and acetic acid (Dwivedy et al. 2018) and hence could be employed as next-generation smart and target-specific delivery vehicle against food biodeterioration. Our result corroborated with the previous finding of Hasheminejad and Khodaiyan (2020) suggesting clove essential oil nanoparticle encapsulated into chitosan nanobiopolymer for postharvest preservation of pomegranate arils against microbial infestation. They described the fungitoxic activity up to 30% by clove essential oil loaded in chitosan nanoparticle over a period of 54 days. Antifungal effects reaching up to 59% by *Schinus molle* essential oil-loaded chitosan nanoemulsion during preservation of corn grains over a period of 15 days of storage has also been recently reported (López-Meneses et al. 2018). However, our finding demonstrated better efficacy (up to 1.5–2.2-fold increase in fungal protection and 100% inhibition of AFB_1) of Nm-AGEO nanoemulsion as compared to the abovementioned investigations. The observed results on improved protection of stored rice seeds against fungal infestation and AFB_1 secretion

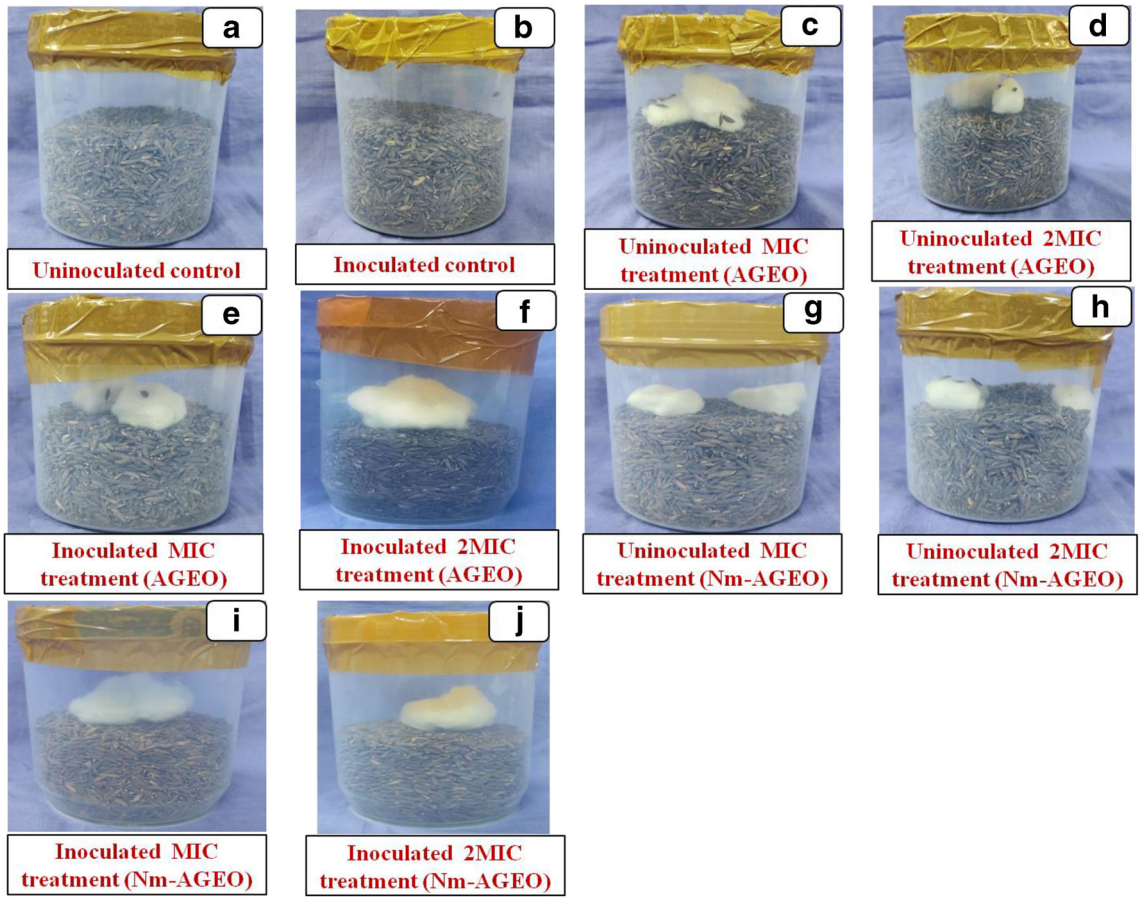

Fig. 5 (**a**–**j**) In situ setup of control as well as different treatment (uninoculated and inoculated) sets by AGEO and Nm-AGEO at MIC and 2 MIC doses on rice samples

up to 1 year of storage periods could be the resultant of controlled release, better antioxidant status, and synergistic activity of AGEO with chitosan nanomatrix in the emulsion droplets after encapsulation.

In addition to fungal and aflatoxin contamination, variable temperature, O_2 sensitivity, and alteration in pH and relative humidity under storage conditions may cause decomposition of rice grain lipid triglycerides (linoleic, oleic, and stearic acids) into free fatty acids (FFAs) such as hydro-peroxides, hydro-aldehydes, 2-octanal, 2-nonenal, and hexanal compounds (Choi et al. 2019). Moderate oxidation of these essential triglycerides causes color change and off-flavor of rice seeds, while excessive oxidation leads to reduced nutritional contents and generation of hydro-peroxide products such as MDA which accelerate the break-down of important cellular proteins (Ghaderi-Ghahfarokhi et al. 2016). Control sets represented higher MDA content (121.36 ± 13.97 μM/gFW), while AGEO and Nm-AGEO fumigation at MIC and 2 MIC concentrations reduced the MDA level up to 109.68 ± 7.49, 92.03 ± 4.54 and 87.12 ± 10.44, 70.23 ± 6.20 μM/g FW, respectively, after 1 year of storage (Fig. 6b). Effective retardation of lipid peroxidation may be due to the presence of antioxidants viz carvone and limonene as the major components of AGEO (Ruberto and Baratta 2000). Moreover, the nanosize of Nm-AGEO and controlled release with effective barrier feature offered by chitosan may significantly inhibit the free radical mediated lipid oxidation in stored rice. Zhang et al. (2019) evaluated the effect of nanomultilayered coating of chitosan matrix incorporated with *Paulownia tomentosa* essential oil on pork chops for effective reduction of MDA level (0.31–2.14 mg MDA/kg) by inhibiting the lipid peroxidation up to 16 days of storage. Encapsulation of clove essential oil into chitosan causing significant decrement of MDA content (< 0.83 mg eq. kg/MDA) during the preservation of frozen tambaqui (*Colossoma macropomum*) facilitated by improvement in the antioxidant activities has been recently reported (Vieira et al. 2019). However, our results demonstrated superior efficacy of Nm-AGEO in protection of rice seeds against the lipid peroxidation of important saturated and unsaturated fatty acids, eventually keeping the very low MDA content up to the storage periods of 1 year that may be explained by reduced rate of respiration which can easily generate the pro-oxidant molecules with lipid hydro-peroxides, thereby suggesting the exciting potential for practical

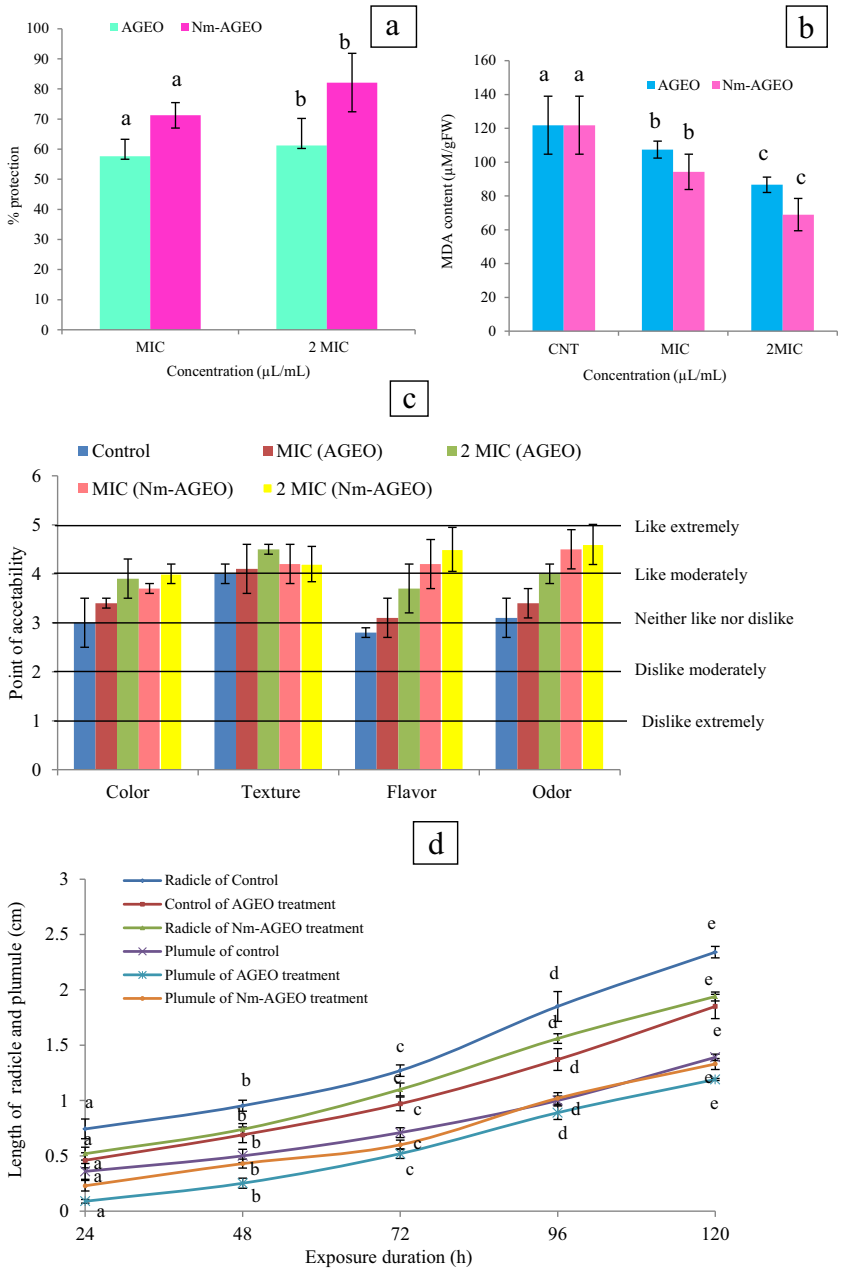

Fig. 6 In situ antifungal efficacy of AGEO and Nm-AGEO on stored rice seeds (**a**), effect of AGEO and Nm-AGEO on lipid peroxidation in stored rice seeds (**b**), effect of AGEO and Nm-AGEO on organoleptic (sensory) properties of stored rice by hedonic scale plot (**c**), and germination test (phytotoxicity assay) of AGEO and Nm-AGEO on stored rice (**d**)

application of Nm-AGEO in food and agricultural industries as green shelf-life enhancer for stored food commodities.

Sensory Attributes of AGEO and Nm-AGEO on Rice Seeds: Evaluation of Organoleptic Property

Sensory attributes (visible appearance of color, texture, flavor, and odor) of rice seeds fumigated with AGEO and Nm-AGEO (MIC and 2 MIC) were evaluated after 1 year of storage and overall acceptability of the rice seeds were determined on hedonic scale (Fig. 6c). Impact of AGEO and Nm-AGEO on color, texture, flavor, and odor of rice seeds should be considered as a key parameter for recommendation as novel green fumigant in food and allied industries. Moreover, the improvement in sensory attributes witnesses the consumer's acceptability and preference. Rice seeds fumigated with AGEO at its MIC dose did not alter color, texture, flavor, and odor, while at 2 MIC dose, marked differences in flavor and odor were noticed making the seeds unacceptable for consumer's willingness that may be due to absorption of higher dose of AGEO by the commodity itself. However, Nm-AGEO-fumigated rice seeds did not show any negative impact on color, texture, flavors, and odor at the 2 MIC dose that could be due to controlled release of aroma. Our result is corroborated with the investigation of Viacava et al. (2018) describing acceptable sensory profile of minimally processed lettuce fumigated

with unencapsulated and microencapsulated *Thymus vulgaris* essential oil under refrigerated condition over 12 days of storage. Another investigation of Martínez-Hernández et al. (2017) demonstrated that carvacrol-loaded chitosan nanoparticle could maintain the acceptable organoleptic properties of fresh cut carrots over a period of 13 days. However, our finding illustrated the better performance of AGEO nanoemulsion in maintenance of organoleptic attributes viz color, texture, flavor, and odor of rice close to the acceptable level during 1 year of storage without any negative impact as reported for chemical preservatives such as potassium meta-bisulfite and sodium benzoate suggesting the suitability and compatibility of encapsulated essential oils application as green shelf-life enhancer.

Phytotoxicity Assay of AGEO and Nm-AGEO-Fumigated Rice Seeds

AGEO and Nm-AGEO-fumigated rice seeds showed good germination with emergence of radicle and plumule within 4–5 days. Both the AGEO and Nm-AGEO did not exhibit any toxic effect on seed germination (Fig. 6d). Phytotoxic effect of chitosan coating incorporated with essential oil during postharvest preservation of strawberry has been demonstrated by Peretto et al. (2017). However, our result contradicted from the previous investigation and affirmed the non-phytotoxic impacts, strengthening the utilization of fumigated seeds for consumption as well as future sowing and intended agricultural practices after large-scale field trial.

Acute Toxicity Assay of AGEO and Nm-AGEO on Mice

Safety assessment of AGEO and Nm-AGEO on mice represented far higher LD_{50} values ($LD_{50\ AGEO}$ = 18,714 μL/kg; $LD_{50\ Nm\text{-}AGEO}$ = 15,987 μL/kg) than frequently used commercial preservatives. Different organophosphate fungitoxicants viz fonophos, tetraethyl-pyrophosphate, and parathion are reported to have very low LD_{50} (1–25 mg/kg) on mammals, thus restricting their wider application in food and agricultural industries. In contrast, botanical preservatives such as azadirachtin (~ 5000 mg/kg) and pyrethrum (300–500 mg/kg) have been reported with lower LD_{50} value (Isman 2006) than AGEO and Nm-AGEO. Hence, higher LD_{50} value together with non-toxic characteristics strengthen the application of AGEO and Nm-AGEO as safe green preservative for large-scale exploitation in food and agricultural industries.

Conclusion

The study reports strong antimicrobial, antiaflatoxigenic, and antioxidant activity of Nm-AGEO as compared to unencapsulated AGEO. The investigation demonstrated biochemical mode of action, mechanism of antifungal activity, and AFB_1 inhibition in terms of reduced ergosterol biosynthesis, destabilization of membrane integrity, efflux of vital cellular ions, and impairment in antioxidant defense molecules (SOD, CAT, GSH/GSSG). The in silico molecular docking deciphered molecular target binding site of carvone and limonene with AFB_1 biosynthesis regulatory genes *Omt-A* and *Ver-1*, implying targeted delivery of encapsulated AGEO. Inhibition of methylglyoxal suggested novel antiaflatoxigenic mechanism of action directing the future exploitation of Nm-AGEO for development of aflatoxin-resistant rice varieties by green transgenic technology. Moreover, strong in situ efficacy, non-phytotoxic nature, negligible mammalian toxicity, and acceptable sensory profile indicated promising application in food systems. Sustained release of encapsulated AGEO from nanostructured chitosan biopolymer demonstrated possibilities in controlled volatilization, thereby considerable improvement in shelf-life of stored food products. In conclusion, the study recommends application of chitosan-fabricated AGEO nanoemulsion in industrial formulation of plant-based safe green food preservative.

Acknowledgements Somenath Das is thankful to the Council of Scientific and Industrial Research (CSIR) [File No.: 09/013(0774)/2018-EMR-I], New Delhi, India, for the financial support. The authors wish to thank the head and coordinator CAS in Botany, DST-FIST, DST-PURSE, ISLS, and CIFC-IIT, Banaras Hindu University (BHU) for laboratory facilities.

Declarations

Conflict of Interest The authors declare no competing interests.

References

Adams, R. P. (2017). *Identification of essential oil components by gas chromatography/mass spectrometry* (Vol. 456). Carol Stream: Allured Publishing Corporation.

Adisa, R. A., Kolawole, N., Sulaimon, L. A., Brai, B., & Ijaola, A. (2019). Alterations of antioxidant status and mitochondrial succinate dehydrogenase activity in the liver of Wistar strain albino rats treated with by ethanol extracts of *Annona senegalensis* Pers (Annonaceae) Stem Bark. *Toxicological Research, 35(1)*, 13–24.

Agnihotri, S. A., Mallikarjuna, N. N., & Aminabhavi, T. M. (2004). Recent advances on chitosan-based micro-and nanoparticles in drug delivery. *Journal of Controlled Release, 100(1)*, 5–28.

Ahmadi, Z., Saber, M., Akbari, A., & Mahdavinia, G. R. (2018). Encapsulation of *Satureja hortensis* L. (Lamiaceae) in chitosan/TPP nanoparticles with enhanced acaricide activity against *Tetranychus urticae* Koch (Acari: Tetranychidae). *Ecotoxicology and Environmental Safety, 161*, 111–119.

Ali, N. (2019). Aflatoxins in rice: worldwide occurrence and public health perspectives. *Toxicology Reports, 6*, 1188–1197.

Amalraj, A., Haponiuk, J. T., Thomas, S., & Gopi, S. (2020). Preparation, characterization and antimicrobial activity of polyvinyl alcohol/gum arabic/chitosan composite films incorporated with black pepper

essential oil and ginger essential oil. *International Journal of Biological Macromolecules, 151*, 366–375.

Amiri, A., Mousakhani-Ganjeh, A., Amiri, Z., Guo, Y. G., Singh, A. P., & Kenari, R. E. (2020). Fabrication of cumin loaded-chitosan particles: characterized by molecular, morphological, thermal, antioxidant, and anticancer properties as well as its utilization in food system. *Food Chemistry, 310*, 125821.

Amjadi, S., Emaminia, S., Nazari, M., Davudian, S. H., Roufegarinejad, L., & Hamishehkar, H. (2019). Application of reinforced ZnO nanoparticle-incorporated gelatin bionanocomposite film with chitosan nanofiber for packaging of chicken fillet and cheese as food models. *Food and Bioprocess Technology, 12*(7), 1205–1219.

Badawy, M. E., Marei, G. I. K., Rabea, E. I., & Taktak, N. E. (2019). Antimicrobial and antioxidant activities of hydrocarbon and oxygenated monoterpenes against some foodborne pathogens through *in vitro* and *in silico* studies. *Pesticide Biochemistry and Physiology, 158*, 185–200.

Bahmankar, M., Mortazavian, S. M. M., Tohidfar, M., Noori, S. A. S., Darbandi, A. I., & Al-fekaiki, D. F. (2019). Chemotypes and morpho-physiological characters affecting essential oil yield in Iranian cumin landraces. *Industrial Crops and Products, 128,* 256–269.

Cao, J. Q., Pang, X., Guo, S. S., Wang, Y., Geng, Z. F., Sang, Y. L., Guo, P. J., & Du, S. S. (2019). Pinene-rich essential oils from *Haplophyllum dauricum* (L.) G. Don display anti-insect activity on two stored-product insects. *International Biodeterioration and Biodegradation, 140*, 1–8.

Chaudhari, A. K., Singh, V. K., Das, S., Singh, B. K., & Dubey, N. K. (2020). Antimicrobial, aflatoxin B_1 inhibitory and lipid oxidation suppressing potential of anethole-based chitosan nanoemulsion as novel preservative for protection of stored maize. *Food and Bioprocess Technology, 13*(8), 1462–1477.

Choi, H., Lee, J., Chang, Y. S., Woo, E. R., & Lee, D. G. (2013). Isolation of (-)-olivil-9′-O-β-d-glucopyranoside from *Sambucus williamsii* and its antifungal effects with membrane-disruptive action. *Biochimica et Biophysica Acta (BBA)-Biomembranes, 1828*(*8*), 2002–2006.

Choi, S., Seo, H. S., Lee, K. R., Lee, S., Lee, J., & Lee, J. (2019). Effect of milling and long-term storage on volatiles of black rice (*Oryza sativa* L.) determined by headspace solid-phase microextraction with gas chromatography–mass spectrometry. *Food Chemistry, 276*, 572–582.

Clemente, I., Aznar, M., & Nerín, C. (2019). Synergistic properties of mustard and cinnamon essential oils for the inactivation of foodborne moulds *in vitro* and on Spanish bread. *International Journal of Food Microbiology, 298*, 44–50.

Da Silva Gündel, S., de Souza, M. E., Quatrin, P. M., Klein, B., Wagner, R., Gündel, A., de Almeida Vaucher, R., Santos, R. C. V., & Ourique, A. F. (2018). Nanoemulsions containing *Cymbopogon flexuosus* essential oil: development, characterization, stability study and evaluation of antimicrobial and antibiofilm activities. *Microbial Pathogenesis, 118*, 268–276.

Dammak, I., Hamdi, Z., El Euch, S. K., Zemni, H., Mliki, A., Hassouna, M., & Lasram, S. (2019). Evaluation of antifungal and anti-ochratoxigenic activities of *Salvia officinalis*, *Lavandula dentata* and *Laurus nobilis* essential oils and a major monoterpene constituent 1, 8-cineole against *Aspergillus carbonarius*. *Industrial Crops and Products, 128*, 85–93.

Das, S., Singh, V. K., Dwivedy, A. K., Chaudhari, A. K., Upadhyay, N., Singh, P., Sharma, S., & Dubey, N. K. (2019). Encapsulation in chitosan-based nanomatrix as an efficient green technology to boost the antimicrobial, antioxidant and *in situ* efficacy of *Coriandrum sativum* essential oil. *International Journal of Biological Macromolecules, 133*, 294–305.

Das, S., Singh, V. K., Dwivedy, A. K., Chaudhari, A. K., Upadhyay, N., Singh, A., Saha, A. K., Ray Chaudhury, S., Prakash, B. & Dubey, N. K. (2020a). Assessment of chemically characterised *Myristica fragrans* essential oil against fungi contaminating stored scented rice and its mode of action as novel aflatoxin inhibitor. *Natural Product Research, 34,* 1611–1615.

Das, S., Singh, V. K., Dwivedy, A. K., Chaudhari, A. K., & Dubey, N. K. (2020b). *Myristica fragrans* essential oil nanoemulsion as novel green preservative against fungal and aflatoxin contamination of food commodities with emphasis on biochemical mode of action and molecular docking of major components. *LWT-Food Science and Technology, 130,* 109495.

Das, S., Singh, V. K., Dwivedy, A. K., Chaudhari, A. K., & Dubey, N. K. (2021a). Nanostructured *Pimpinella anisum* essential oil as novel green food preservative against fungal infestation, aflatoxin B_1 contamination and deterioration of nutritional qualities. *Food Chemistry, 344,* 128574.

Das, S., Singh, V. K., Dwivedy, A. K., Chaudhari, A. K., & Dubey, N. K. (2021b). Eugenol loaded chitosan nanoemulsion for food protection and inhibition of aflatoxin B_1 synthesizing genes based on molecular docking. *Carbohydrate Polymers, 255,* 117339.

Dubey, N. K., Kumar, A., & Kumar, A. (2017). Efficacy of *Luvunga scandens* Roxb. essential oil as antifungal, aflatoxin suppressor and antioxidant. *Journal of Food Technology and Preservation, 1*, 37–41.

Dwivedy, A. K., Singh, V. K., Prakash, B., & Dubey, N. K. (2018). Nanoencapsulated *Illicium verum* Hook. f. essential oil as an effective novel plant-based preservative against aflatoxin B_1 production and free radical generation. *Food and Chemical Toxicology, 111*, 102–113.

Esmaeili, A., & Asgari, A. (2015). *In vitro* release and biological activities of *Carum copticum* essential oil (CEO) loaded chitosan nanoparticles. *International Journal of Biological Macromolecules, 81*, 283–290.

Ezhilarasi, P. N., Karthik, P., Chhanwal, N., & Anandharamakrishnan, C. (2013). Nanoencapsulation techniques for food bioactive components: a review. *Food and Bioprocess Technology, 6*(3), 628–647.

Feyzioglu, G. C., & Tornuk, F. (2016). Development of chitosan nanoparticles loaded with summer savory (*Satureja hortensis* L.) essential oil for antimicrobial and antioxidant delivery applications. *LWT-Food Science and Technology, 70*, 104–110.

Ghaderi-Ghahfarokhi, M., Barzegar, M., Sahari, M. A., & Azizi, M. H. (2016). Nanoencapsulation approach to improve antimicrobial and antioxidant activity of thyme essential oil in beef burgers during refrigerated storage. *Food and Bioprocess Technology, 9*(7), 1187–1201.

Gómez-Pastora, J., Bringas, E., & Ortiz, I. (2014). Recent progress and future challenges on the use of high performance magnetic nano-adsorbents in environmental applications. *Chemical Engineering Journal, 256*, 187–204.

Grintzalis, K., Vernardis, S. I., Klapa, M. I., & Georgiou, C. D. (2014). Role of oxidative stress in sclerotial differentiation and aflatoxin B_1 biosynthesis in *Aspergillus flavus*. *Applied and Environmental Microbiology, 80*(18), 5561–5571.

Hadidi, M., Pouramin, S., Adinepour, F., Haghani, S., & Jafari, S. M. (2020). Chitosan nanoparticles loaded with clove essential oil: characterization, antioxidant and antibacterial activities. *Carbohydrate Polymers, 236,* 116075.

Hasani, S., Ojagh, S. M., & Ghorbani, M. (2018). Nanoencapsulation of lemon essential oil in Chitosan-Hicap system. Part 1: study on its physical and structural characteristics. *International Journal of Biological Macromolecules, 115*, 143–151.

Hasheminejad, N., & Khodaiyan, F. (2020). The effect of clove essential oil loaded chitosan nanoparticles on the shelf life and quality of pomegranate arils. *Food Chemistry, 309*, 125520.

Hasheminejad, N., Khodaiyan, F., & Safari, M. (2019). Improving the antifungal activity of clove essential oil encapsulated by chitosan nanoparticles. *Food Chemistry, 275*, 113–122.

Hemmatkhah, F., Zeynali, F., & Almasi, H. (2020). Encapsulated cumin seed essential oil-loaded active papers: characterization and evaluation of the effect on quality attributes of beef hamburger. *Food and Bioprocess Technology, 13*(3), 533–547.

Hosseini, S. F., Zandi, M., Rezaei, M., & Farahmandghavi, F. (2013). Two-step method for encapsulation of oregano essential oil in chitosan nanoparticles: preparation, characterization and *in vitro* release study. *Carbohydrate Polymers, 95*(*1*), 50–56.

Hussain, M. R., & Maji, T. K. (2008). Preparation of genipin cross-linked chitosan-gelatin microcapsules for encapsulation of *Zanthoxylum limonella* oil (ZLO) using salting-out method. *Journal of Microencapsulation, 25*(*6*), 414–420.

Isman, M. B. (2006). Botanical insecticides, deterrents, and repellents in modern agriculture and an increasingly regulated world. *Annual Review of Entomology, 51*(1), 45–66.

Jiang, Y., Lan, W., Sameen, D. E., Ahmed, S., Qin, W., Zhang, Q., Chen, H., Dai, J., He, L., & Liu, Y. (2020). Preparation and characterization of grass carp collagen-chitosan-lemon essential oil composite films for application as food packaging. *International Journal of Biological Macromolecules, 160*, 340–351.

Kalagatur, N. K., Nirmal Ghosh, O. S., Sundararaj, N., & Mudili, V. (2018). Antifungal activity of chitosan nanoparticles encapsulated with *Cymbopogon martinii* essential oil on plant pathogenic fungi *Fusarium graminearum*. *Frontiers in Pharmacology, 9*, 610.

Karam, T. K., Ortega, S., Nakamura, T. U., Auzély-Velty, R., & Nakamura, C. V. (2020). Development of chitosan nanocapsules containing essential oil of *Matricaria chamomilla* L. for the treatment of cutaneous leishmaniasis. *International Journal of Biological Macromolecules, 162*, 199–208.

Kaur, N., Chahal, K. K., Kumar, A., Singh, R., & Bhardwaj, U. (2019). Antioxidant activity of *Anethum graveolens* L. essential oil constituents and their chemical analogues. *Journal of Food Biochemistry*, *43(4)*, e12782.

Kong, J., Zhang, Y., Ju, J., Xie, Y., Guo, Y., Cheng, Y., & Yao, W. (2019). Antifungal effects of thymol and salicylic acid on cell membrane and mitochondria of *Rhizopus stolonifer* and their application in postharvest preservation of tomatoes. *Food Chemistry, 285*, 380–388.

Kou, X. H., Guo, W. L., Guo, R. Z., Li, X. Y., & Xue, Z. H. (2014). Effects of chitosan, calcium chloride, and pullulan coating treatments on antioxidant activity in pear cv."Huang guan" during storage. *Food and Bioprocess Technology, 7*(3), 671–681.

Liu, K., Li, Y., Chen, F., & Yong, F. (2017). Lipid oxidation of brown rice stored at different temperatures. *International Journal of Food Science and Technology, 52*(1), 188–195.

Liu, Y., Tang, T., Duan, S., Qin, Z., Zhao, H., Wang, M., Li, C., Zhang, Z., Liu, A., Han, G., & Wu, D. (2020). Applicability of rice doughs as promising food materials in extrusion-based 3D printing. *Food and Bioprocess Technology, 13*(3), 548–563.

López-Meneses, A. K., Plascencia-Jatomea, M., Lizardi-Mendoza, J., Fernández-Quiroz, D., Rodríguez-Félix, F., Mouriño-Pérez, R. R., & Cortez-Rocha, M. O. (2018). *Schinus molle* L. essential oil-loaded chitosan nanoparticles: preparation, characterization, antifungal and anti-aflatoxigenic properties. *LWT-Food Science and Technology, 96*, 597–603.

Lowry, O. H., Rosebrough, N. J., Farr, A. L., & Randall, R. J. (1951). Measurement of protein with the Folin phenol reagent. *Journal of Biological Chemistry, 193*(1), 265–275.

Lv, C., Wang, P., Ma, L., Zheng, M., Liu, Y., & Xing, F. (2018). Large-scale comparative analysis of eugenol-induced/repressed genes expression in *Aspergillus flavus* using RNA-seq. *Frontiers in Microbiology, 9*, 1116.

Martínez-Hernández, G. B., Amodio, M. L., & Colelli, G. (2017). Carvacrol-loaded chitosan nanoparticles maintain quality of fresh-cut carrots. *Innovative Food Science and Emerging Technologies, 41*, 56–63.

Molamohammadi, H., Pakkish, Z., Akhavan, H. R., & Saffari, V. R. (2020). Effect of salicylic acid incorporated chitosan coating on shelf life extension of fresh in-hull pistachio fruit. *Food and Bioprocess Technology, 13*(1), 121–131.

Motwani, S. K., Chopra, S., Talegaonkar, S., Kohli, K., Ahmad, F. J., & Khar, R. K. (2008). Chitosan–sodium alginate nanoparticles as submicroscopic reservoirs for ocular delivery: formulation, optimisation and *in vitro* characterisation. *European Journal of Pharmaceutics and Biopharmaceutics, 68*(*3*), 513–525.

Murugan, K., Anandaraj, K., & Al-Sohaibani, S. (2013). Antiaflatoxigenic food additive potential of *Murraya koenigii*: an *in vitro* and molecular interaction study. *Food Research International, 52*(*1*), 8–16.

Oliveira, É. R., Fernandes, R. V., Botrel, D. A., Carmo, E. L., Borges, S. V., & Queiroz, F. (2018). Study of different wall matrix biopolymers on the properties of spray-dried pequi oil and on the stability of bioactive compounds. *Food and Bioprocess Technology, 11*(3), 660–679.

Peretto, G., Du, W. X., Avena-Bustillos, R. J., Berrios, J. D. J., Sambo, P., & McHugh, T. H. (2017). Electrostatic and conventional spraying of alginate-based edible coating with natural antimicrobials for preserving fresh strawberry quality. *Food and Bioprocess Technology, 10*(1), 165–174.

Pinto, E., Pina-Vaz, C., Salgueiro, L., Gonçalves, M. J., Costa-de-Oliveira, S., Cavaleiro, C., Palmeira, A., Rodrigues, A., & Martinez-de-Oliveira, J. (2006). Antifungal activity of the essential oil of *Thymus pulegioides* on *Candida*, *Aspergillus* and dermatophyte species. *Journal of Medical Microbiology, 55*(*10*), 1367–1373.

Porep, J. U., Mrugala, S., Nikfardjam, M. S. P., & Carle, R. (2015). Online determination of ergosterol in naturally contaminated grape mashes under industrial conditions at wineries. *Food and Bioprocess Technology, 8*(7), 1455–1464.

Radhakrishnan, V. S., Mudiam, M. K. R., Kumar, M., Dwivedi, S. P., Singh, S. P., & Prasad, T. (2018). Silver nanoparticles induced alterations in multiple cellular targets, which are critical for drug susceptibilities and pathogenicity in fungal pathogen (*Candida albicans*). *International Journal of Nanomedicine, 13*, 2647–2663.

Rajkumar, V., Gunasekaran, C., Dharmaraj, J., Chinnaraj, P., Paul, C. A., & Kanithachristy, I. (2020). Structural characterization of chitosan nanoparticle loaded with Piper nigrum essential oil for biological efficacy against the stored grain pest control. *Pesticide Biochemistry and Physiology, 166,* 104566.

Ruberto, G., & Baratta, M. T. (2000). Antioxidant activity of selected essential oil components in two lipid model systems. *Food Chemistry, 69*(2), 167–174.

Ruiz-Navajas, Y., Viuda-Martos, M., Sendra, E., Perez-Alvarez, J. A., & Fernández-López, J. (2013). *In vitro* antibacterial and antioxidant properties of chitosan edible films incorporated with *Thymus moroderi* or *Thymus piperella* essential oils. *Food Control, 30*(*2*), 386–392.

Shah, B. R., Li, Y., Jin, W., An, Y., He, L., Li, Z., Xu, W., & Li, B. (2016). Preparation and optimization of Pickering emulsion stabilized by chitosan-tripolyphosphate nanoparticles for curcumin encapsulation. *Food Hydrocolloids, 52*, 369–377.

Shao, X., Cheng, S., Wang, H., Yu, D., & Mungai, C. (2013). The possible mechanism of antifungal action of tea tree oil on *Botrytis cinerea*. *Journal of Applied Microbiology, 114*(*6*), 1642–1649.

Sharifimehr, S., Soltanizadeh, N., & Hossein Goli, S. A. (2019). Effects of edible coating containing nano-emulsion of *Aloe vera* and eugenol on the physicochemical properties of shrimp during cold storage. *Journal of the Science of Food and Agriculture, 99*(*7*), 3604–3615.

Shetta, A., Kegere, J., & Mamdouh, W. (2019). Comparative study of encapsulated peppermint and green tea essential oils in chitosan nanoparticles: encapsulation, thermal stability, *in-vitro* release,

antioxidant and antibacterial activities. *International Journal of Biological Macromolecules, 126*, 731–742.

Singh, V. K., Das, S., Dwivedy, A. K., Rathore, R., & Dubey, N. K. (2019). Assessment of chemically characterized nanoencapuslated *Ocimum sanctum* essential oil against aflatoxigenic fungi contaminating herbal raw materials and its novel mode of action as methyglyoxal inhibitor. *Postharvest Biology and Technology, 153*, 87–95.

Sun, Q., Shang, B., Wang, L., Lu, Z., & Liu, Y. (2016). Cinnamaldehyde inhibits fungal growth and aflatoxin B_1 biosynthesis by modulating the oxidative stress response of *Aspergillus flavus*. *Applied Microbiology and Biotechnology, 100*(3), 1355–1364.

Tian, J., Huang, B., Luo, X., Zeng, H., Ban, X., He, J., & Wang, Y. (2012). The control of *Aspergillus flavus* with *Cinnamomum jensenianum* Hand.-Mazz essential oil and its potential use as a food preservative. *Food Chemistry, 130*(3), 520–527.

Upadhyay, N., Singh, V. K., Dwivedy, A. K., Das, S., Chaudhari, A. K., & Dubey, N. K. (2018). *Cistus ladanifer* L. essential oil as a plant based preservative against molds infesting oil seeds, aflatoxin B_1 secretion, oxidative deterioration and methylglyoxal biosynthesis. *LWT- Food Science and Technology, 92*, 395–403.

Usha, T., Goyal, A. K., Lubna, S., Prashanth, H., Mohan, T. M., Pande, V., & Middha, S. K. (2014). Identification of anti-cancer targets of eco-friendly waste *Punica granatum* peel by dual reverse virtual screening and binding analysis. *Asian Pacific Journal of Cancer Prevention, 15*(23), 10345–10350.

Viacava, G. E., Ayala-Zavala, J. F., González-Aguilar, G. A., & Ansorena, M. R. (2018). Effect of free and microencapsulated thyme essential oil on quality attributes of minimally processed lettuce. *Postharvest Biology and Technology, 145*, 125–133.

Vieira, B. B., Mafra, J. F., da Rocha Bispo, A. S., Ferreira, M. A., de Lima Silva, F., Rodrigues, A. V. N., & Evangelista-Barreto, N. S. (2019). Combination of chitosan coating and clove essential oil reduces lipid oxidation and microbial growth in frozen stored tambaqui (*Colossoma macropomum*) fillets. *LWT-Food Science and Technology, 116*, 108546.

Wang, Y., Xia, Y., Zhang, P., Ye, L., Wu, L., & He, S. (2017). Physical characterization and pork packaging application of chitosan films incorporated with combined essential oils of cinnamon and ginger. *Food and Bioprocess Technology, 10*(3), 503–511.

Weydert, C. J., & Cullen, J. J. (2010). Measurement of superoxide dismutase, catalase and glutathione peroxidase in cultured cells and tissue. *Nature Protocols, 5*(*1*), 51–66.

Woranuch, S., & Yoksan, R. (2013). Eugenol-loaded chitosan nanoparticles: I. Thermal stability improvement of eugenol through encapsulation. *Carbohydrate Polymers, 96*(2), 578–585.

Yadav, S. K., Singla-Pareek, S. L., Ray, M., Reddy, M. K., & Sopory, S. K. (2005). Methylglyoxal levels in plants under salinity stress are dependent on glyoxalase I and glutathione. *Biochemical and Biophysical Research Communications, 337*(*1*), 61–67.

Yang, H., Tong, J., Lee, C. W., Ha, S., Eom, S. H., & Im, Y. J. (2015). Structural mechanism of ergosterol regulation by fungal sterol transcription factor Upc2. *Nature Communications, 6*(*1*), 1–13.

Yili, A., Yimamu, H., Maksimov, V. V., Aisa, H. A., Veshkurova, O. N., & Salikhov, S. I. (2006). Chemical composition of essential oil from seeds of *Anethum graveolens* cultivated in China. *Chemistry of Natural Compounds, 42*(*4*), 491–492.

Zhang, H., Li, X., & Kang, H. (2019). Chitosan coatings incorporated with free or nano-encapsulated *Paulownia tomentosa* essential oil to improve shelf-life of ready-to-cook pork chops. *LWT-Food Science Technology, 116*, 108580.

Zheng, F., Zheng, W., Li, L., Pan, S., Liu, M., Zhang, W., Liu, H., & Zhu, C. (2017). Chitosan controls postharvest decay and elicits defense response in kiwifruit. *Food and Bioprocess Technology, 10*(11), 1937–1945.